

THESIS

EFFECT OF MOUNTAIN PINE BEETLE KILL ON STREAMFLOW GENERATION MECHANISMS

Submitted by

Christine Elisabeth Wehner

Department of Ecosystem Science and Sustainability

In partial fulfillment of the requirements

For the Degree of Master of Science

Colorado State University

Fort Collins, Colorado

Summer, 2016

Master's Committee:

Advisor: John D. Stednick

Steven R. Fassnacht
Jeffrey Niemann

Copyright by Christine Elisabeth Wehner 2016

All Rights Reserved

ABSTRACT

EFFECT OF MOUNTAIN PINE BEETLE KILL ON STREAMFLOW GENERATION MECHANISMS

The mountain pine beetle (*Dendroctonus ponderosae*) is an endemic species to Colorado, but a recent epidemic resulted in the mortality of millions of acres of lodgepole pine forest in Colorado since 2002. This study examined the effect of the mountain pine beetle kill on streamflow generation mechanisms using different tracer methods. Eleven nested watersheds with varying level of beetle-killed forest area (47.1% to 97.4%) were chosen for study. Groundwater, surface water, and precipitation samples were taken and analyzed for stable isotope composition (^2H and ^{18}O), specific conductivity, and chloride concentrations.

Four methods were employed to partition sources of streamflow, or streamflow generation mechanisms (SGM), in beetle-killed watersheds. Stable isotopes (^2H and ^{18}O) were used to determine mean fractional contribution of each source (groundwater, rain, and snow) to streamflow. Rain and snow contribution were negatively correlated with beetle-killed forest area ($p=0.08$ and $p=0.35$ respectively). Groundwater was positively correlated with increasing beetle-killed forest area ($p=0.23$). Specific conductivity and chloride were each used in a 2-component (groundwater and precipitation) hydrograph separation. Using specific conductivity, beetle kill was negatively correlated with average groundwater contribution ($\rho = -0.13$), but the result was not significant ($p = 0.71$). Using chloride, the results were correlated ($\rho=0.19$), but not significant ($p = 0.58$). Specific conductivity and chloride measurements were then coupled in a 3-component (groundwater, rain, and snow) end member mixing analysis (EMMA). Beetle-killed forest area and fractional groundwater contribution were positively correlated ($\rho=0.26$), but not significant ($p = 0.43$). Watershed characteristics were examined to determine potential metrics of groundwater contribution. Mean watershed elevation displayed a significant negative correlation with mean groundwater contribution ($p = 0.08$).

ACKNOWLEDGEMENTS

This work is the result of the help and advice of many people. Firstly, I would like to thank my advisor, Dr. John Stednick, for his indispensable guidance and encouragement throughout the pursuit of my master's degree. I would like to acknowledge Dr. Steven R. Fassnacht and Dr. Jeffrey Niemann for taking time out of their busy schedules to serve as my committee members and provide valuable feedback. Funding for this project was made available by the National Science Foundation grant: Water Quality and Supply Impacts from Climate-Induced Insect Tree Mortality.

I would also like to thank my friends and fellow graduate students for their support, particularly Anna Pfohl for her help with data collection in the field. Finally, I would like to thank my family, John, Ann, and Katie Wehner, for their unwavering support of my education.

TABLE OF CONTENTS

ABSTRACT	ii
ACKNOWLEDGEMENTS.....	iii
LIST OF TABLES.....	v
LIST OF FIGURES	vi
INTRODUCTION.....	1
Timber Harvesting: Streamflow Generation Mechanisms	2
Mountain Pine Beetle: Streamflow Generation Mechanisms.....	3
Stable Isotope Hydrology.....	5
Chemical Hydrograph Separation	8
<i>Specific Conductivity</i>	9
<i>Chloride</i>	10
<i>End Member Mixing Analysis (EMMA)</i>	10
HYPOTHESIS AND STUDY OBJECTIVES:	12
METHODS.....	13
Site Description:.....	13
Isotopy.....	16
Chemical Hydrograph Separation	18
<i>Specific Conductivity</i>	18
<i>Chloride</i>	18
<i>End Member Mixing Analysis (EMMA)</i>	20
RESULTS AND DISCUSSION.....	21
Isotopy.....	21
Chemical Hydrograph Separation	28
<i>Specific Conductivity</i>	28
<i>Chloride</i>	31
<i>End Member Mixing Analysis (EMMA)</i>	31
Chemical Hydrograph Separation Discussion.....	33
<i>Specific Conductivity</i>	33
<i>Chloride</i>	34
<i>End Member Mixing Analysis (EMMA)</i>	35
Watershed Physiography.....	37
CONCLUSIONS	39
RECOMMENDATIONS.....	40
LITERATURE CITED.....	41
APPENDIX	47

LIST OF TABLES

Table 1. Watershed names, site ID, watershed area, average elevation, and percent of total watershed area affected by the mountain pine beetle for each site.	14
Table 2. Difference between mean groundwater and surface water isotope compositions and associated two-tailed p-values.....	23
Table 3. Mean source water contributions for each study conducted using stable isotopes (2H and 18O) in the Rocky Mountains of North-Central Colorado.	27
Table 4. Source water contributions for each study period at Willow Creek above the Reservoir (WCR), resampled for dates between April and October and re-analyzed using SIAR.	27
Table 5. Difference between mean groundwater and surface water specific conductivity ($\mu\text{S}/\text{cm}$) and chloride concentration (mg/L) with a two-tailed p-value for each site.....	28
Table 6. Watershed characteristics and correlation with fractional groundwater contribution.....	37

LIST OF FIGURES

Figure 1. Mean source water contribution vs. cumulative beetle-killed area for 17 watersheds in Grand, Eagle, and Summit County, Colorado (from Menger, 2015). 8

Figure 2. Watershed location (above), site locations (right), and beetle kill extent (left) in Willow Creek Watershed, Grand County, CO..... 15

Figure 3. Isotopic composition of source waters (a) including precipitation data collected from 2011 to 2015 with a LMWL for the Colorado Rocky Mountains (Menger, 2015) and b.) groundwater and surface water isotope compositions for all of the sites during water year 2015, plotted with the LMWL (Menger, 2015). 23

Figure 4. Average rain, snow, and groundwater contribution to streamflow vs. beetle-killed forest area (%) for 5 subwatersheds in Willow Creek watershed from April-October 2015. 24

Figure 5. Rain, snow, and groundwater contribution to streamflow at Willow Creek above Reservoir (WCR) over the sampling season. 24

Figure 6. Snow water equivalent, temperature, and precipitation over the 2015 water year. SnoTEL site 869 historical daily data (NRCS, 2015). Temperature data from GRAND LAKE 6 SSW station (<http://www.ncdc.noaa.gov/>). The extent of Figure 5 is shown in grey..... 25

Figure 7. Fractional groundwater contribution vs. beetle kill forest area (%) using specific conductivity ($\rho=-0.13$, $p=0.71$), chloride ($\rho=0.19$, $p=0.58$), and end member mixing analysis ($\rho=0.26$, $p=0.43$). 29

Figure 8. Fractional groundwater contribution and discharge for each sampling date at WCR using each tracer method. 30

Figure 9. Mixing diagram for WCR including the specific conductivity and chloride concentrations of each source and the stream (shown on a log scale). 33

Figure 10. Fractional source contribution vs. elevation (m) for 5 watersheds in Willow Creek. 38

Figure 11. Mean elevation vs. beetle-killed forest area for 5 sub-watersheds assessed for isotopic composition. 38

INTRODUCTION

The mountain pine beetle (*Dendroctonus ponderosae*), an endemic species to western North America, has increased in population to epidemic levels in the Rocky Mountains, killing extensive areas of lodgepole pine (*Pinus contorta*) forests from 2002 to 2012. Between 1996 and 2013, the mountain pine beetle killed approximately 3.4 million acres of forest in Colorado (CSFS, 2014). Bark beetle activity increases when critical thresholds have been breached, which may be intensified by climate change, drought, and warmer winter temperatures (Raffa et al., 2008). While mountain pine beetle populations have been decreasing in Colorado due to lack of host trees (CSFS, 2014), it is important to understand the effect of the mountain pine beetle kill on water resources of the west.

The process that brings about tree mortality is a blue stain fungi (*Grosmannia claviger*) in the xylem tissue that transports water from the roots to the canopy (Hubbard et al., 2013). The mountain pine beetle carries this fungus, called “blue stain” due to the color it causes in beetle-killed wood, infecting the tree when it creates bore holes to feed on phloem (Ballard et al., 1984). After bark beetle infestation, a pine tree will undergo three distinct phases with different hydrological implications. During the year when needles are green, the tree will transpire, drawing water from the root zone, and the canopy will intercept precipitation and shade the ground (Wulder et al., 2006; Mikkelsen et al., 2013a). Next is the red phase where the needles turn red but remain on the tree, and transpiration has ceased. After approximately 3-5 years, the tree will enter the grey phase and drop its needles (Wulder et al., 2006). After the grey phase, trees begin to fall, which can begin 5 to 14 years after infestation (Mitchell and Preisler, 1998), although the timing of tree fall may depend on soil moisture conditions and weather events (Lewis and Hartley, 2006; Wulder et al., 2006; Klutsch et al., 2009). Within the first few years after needle drop, light becomes more available due to reduced canopy, beginning forest regeneration (Collins et al., 2011).

Many of the forested watersheds affected by the beetle kill are important drinking and irrigation water sources for the North American west, where water resources are highly valued. The mountain pine beetle may affect the hydrology of infested watersheds due to changes in water uptake and canopy cover. Studies on tree harvesting show increases in water yield after vegetation loss or removal (Stednick, 1996; Surfleet and Skaugset, 2013). Similarly, the loss of transpiration associated with bark beetle infestation results in increased streamflow. Early studies have shown that forested watersheds affected by bark beetles can result in increased water yield. The first

study on streamflow response to beetle infestation indicated increases in streamflow due to beetle infestation in the White River (infested) compared to the Elk River (healthy) (Love, 1955). The White River had experienced about 60% forest mortality. Paired-watershed analysis of streamflow for a 25-year period (1941-1965) showed increased streamflow and peak flow (Bethlahmy, 1974). Including the Yampa River in the analysis showed that the White and Yampa rivers both yielded more stream flow than expected, and the largest increases occurred 15 years after infestation (Bethlahmy, 1974).

Early studies on bark beetle infestation suggest increases in water yield following infestation, but these studies did not explore streamflow generation mechanisms. Timber harvesting, which involves tree removal, may be a helpful paradigm to predict changes in streamflow generation mechanisms following bark beetle-kill.

Timber Harvesting: Streamflow Generation Mechanisms

Other types of vegetation loss, such as tree harvesting, and corresponding changed streamflow generation mechanisms have been highly studied and may reveal information about beetle killed watersheds. The vegetation removal associated with timber harvesting brings about changes in the hydrologic cycle, affecting streamflow generation mechanisms.

Tree removal from timber harvest brings about a decrease in canopy cover and decreasing interception (Keppeler, 1998; Roth et al., 2007). Timber harvest also brings about a reduction in transpiration and increases in soil evaporation due to increased solar radiation from the reduced canopy (Sun et al., 2001). The net result of these changes is an increase in groundwater level after timber harvest. Observed increases in summer low flows after timber harvest may be attributed to groundwater (Hornbeck, 1993; Hornbeck 1997). Increased peak flows are apparent after timber harvesting in snowmelt-dominated watersheds (Troendle and King, 1985). Increases in SWE from decreased canopy sublimation are partially offset by increased solar radiation (Stednick, 1996). In total, tree harvesting has increased annual stream flows, peak flows, and annual snowpack (SWE) (Troendle and King, 1985; Troendle and King, 1987; Troendle and Reuss, 1997) and an increase in snowmelt rate (Murray and Buttle, 2003). In the Rocky Mountain region, as little as 15% of forest basal area removed can generate an observable response in annual water yield (Stednick, 1996).

Similarities between MPB and tree harvesting include decreases in canopy cover, interception, and transpiration. MPB-killed forests may show similar changes to the hydrologic cycle. However, recent studies have suggested that the hydrologic response to beetle kill may be different from that of timber harvesting (Bearup et al., 2014; Maggart, 2014; Menger, 2015). Streamflow changes resulting from the mountain pine beetle occur over the course of a few years, while the effects of tree harvesting are immediate (Pugh and Gordon, 2013). In addition, tree harvesting involves removal of the tree bole, while the beetle kill leaves the tree intact. Logging operations often include soil disturbance from compaction and road construction (Adams et al., 2012; Mikkelson et al., 2013b). Bark beetles also tend to affect forests over larger temporal and spatial scales than forest fires or logging (Bearup et al., 2014). As a result, tree harvesting and mountain pine beetle-killed trees affect the water and energy budgets differently. In order to draw conclusions about the mountain pine beetle infestation's effect on hydrology, it is necessary to study bark-beetle infested forests.

Mountain Pine Beetle: Streamflow Generation Mechanisms

Tree mortality resulting from with the mountain pine beetle infestation brings about changes in hydrologic processes. Changes in the water and energy budget due to cessation of transpiration and canopy loss affect groundwater levels, snowpack, and snowmelt. Drawing conclusions about these processes and their effects on streamflow generation at the watershed scale may be difficult at the watershed scale.

Soil water will increase under the grey phase due to increased infiltration from forest litter (Martin and Moody, 2001) in addition to increased water availability from decreased evapotranspiration and interception (Pugh and Gordon, 2013). Increases in surface evaporation also occur as a result of canopy loss (Mikkelson et al., 2013b; Biederman et al., 2014). However, modeling studies predict decreases in overall evapotranspiration (Chen et al., 2015) and increases in soil moisture (Mikkelson et al., 2013b). Field studies confirm predicted increases in soil moisture (Clow et al., 2011), but changes may only be significant in summer months (Moorehouse et al., 2008). These effects will result in increases in overall groundwater storage, as more water reaches the soil surface and less water is taken up by vegetation. In addition, the decreased canopy cover will bring about increased evaporative loss from the soil surface due to increases in solar radiation that reaches the surface. This may result in decreased soil moisture and depleted groundwater levels, but most studies report overall increases in groundwater levels after bark beetle infestation. In the forest regeneration stage, however, transpiration rates increase, resulting in lower

groundwater levels, soil moisture (Pugh and Gordon, 2013; Bearup et al., 2014), and water yields (Linveh et al., 2015). Thus, predicting responses using energy and water budgets becomes complicated. As a result, it may be helpful to use isotopic and chemical tracer techniques to quantify streamflow generation mechanisms as relative source contribution to streamflow in beetle-killed watersheds.

Snowpack snow water equivalent (SWE) will increase after canopy loss resulting from the bark beetle kill. The snowpack will lose less to canopy sublimation due to the decrease in canopy interception (Boon, 2011; Pugh and Small, 2012; Pugh and Gordon, 2013). However, wind energy, which can increase surface sublimation rates, will increase as the canopy and stand is lost until regeneration, increasing snowpack ablation (Bergen, 1971). Overall, snow accumulation increases in bark beetle-killed forests due to decreased canopy interception (Boon, 2011; Mikkelsen et al., 2013a). However, in some cases, increased snow ablation may offset increased snow accumulation (Biederman et al., 2012; Pugh and Small, 2012).

The tree canopy controls incoming solar radiation to the forest floor (Perrot et al., 2014). Snowmelt is largely controlled by this energy input as well as the surface albedo of the snow, which is affected by forest debris or litter (Pugh and Gordon, 2013). Albedo will decrease during the red phase due to the dropping of needles and increase in the grey and tree fall phase. Therefore, snowmelt energy will increase gradually after the green phase due to loss of canopy (Pugh and Gordon, 2013; Mikkelsen et al., 2013a). Due to the changes in canopy structure, snowmelt occurs sooner in beetle-killed forests, resulting in an earlier date of peak flow (Perrot et al., 2014). In the headwaters of the Colorado River in north central Colorado, snowpack ablation occurred one week earlier in red phase stands compared to living stands (Pugh and Small, 2012). In the Jack Creek watershed in southwestern MT, snow melt rate also advanced one to two weeks due to reduced soil moisture deficit and reductions in canopy cover (Potts, 1984).

Total basin response to beetle kill proves to be more difficult to generalize than tree-scale processes (Adams et al., 2012; Mikkelsen et al., 2013b). Early paired watershed studies indicated an increase in annual water yield in watersheds affected by bark beetles (Love, 1955; Bethlahmy, 1974). However, other attempts to detect changes in the hydrology and energy budget of a beetle-killed watershed suggest that it may be more complicated than the conceptual response suggests. A double-mass analysis in Jack Creek watershed (southwestern Montana) after a mountain pine beetle epidemic that ranged from 50 to 60% mortality among commercial timber and 35%

mortality in the total growing stock showed a 15% increase in water yield, but this result was not significant (Potts, 1984).

Some recent studies on the western slope of the Rocky Mountains in Colorado also found that bark beetle infestation has no significant correlation with fractional groundwater contribution (Maggart, 2014; Menger, 2015). Analysis of peak flow, date of peak flow, and annual water yield in 21 watersheds all displayed stationarity, even after a watershed was infested with bark beetles (Maggart, 2014). However, other recent research in the Colorado Rocky Mountains suggest increases in annual water yield between 8 and 13% due to greater snow accumulation and decreased overall evapotranspiration (Linveh et al., 2015). In addition, annual mean relative contributions of snow, rain, and groundwater measured by isotopy were not significantly affected by degree of beetle kill (by area) (Maggart, 2014; Menger, 2015).

Stable Isotope Hydrology

Stable isotopes may provide information about streamflow response in beetle-killed watersheds. Stable isotopes as hydrologic tracers can reveal information about the origin and processes that have acted upon surface waters (Faure and Mensing, 2005). Stable, heavy isotopes of oxygen and hydrogen, ^{18}O and ^2H , can act as conservative tracers for determining the relative contribution of different source waters. This analysis relies on the mechanism of isotopic fractionation, in which different reservoirs of water undergo processes that alter the isotope composition. As a result, in a given region, groundwater, precipitation as rain, and precipitation as snow will have distinct ^2H and ^{18}O isotopic composition (Faure and Mensing, 2005). In addition ^{18}O and ^2H are referred to as environmental tracers, meaning that they are present in the environment and there is no experimental control over their presence, but they still can reveal important information about the mechanisms involved in streamflow generation (Gupta, 2010).

The isotopic enrichment of ^2H and ^{18}O are commonly measured relative to the Standard Mean Ocean Water (SMOW) and reported in units of per mil (‰) (Craig, 1961). The $\delta^2\text{H}$ and $\delta^{18}\text{O}$ values of meteoric precipitation are both negative, meaning that SMOW is more enriched in the heavy isotopes than meteoric waters (Faure and Mensing, 2005). Enrichment can be calculated using equation 1 (Dansgaard, 1964).

$$\delta = \frac{R_{sample} - R_{SMOW}}{R_{SMOW}} * 10^3 \text{‰}$$

Equation 1

Where δ , expressed in per mil, is the enrichment of a particular isotope relative to a standard, R_{sample} is the isotope ratio of the sample and R_{SMOW} is the isotope ratio of standard mean ocean water (SMOW). Unless excessive evaporation has occurred, this enrichment follows a predictable linear pattern called the Global Meteoric Water Line (GMWL), which provides a relation between ^2H and ^{18}O for meteoric waters around the world (Equation 2) (Craig, 1961).

$$\delta^2\text{H} = 8\delta\text{O}^{18} + 10$$

Equation 2

Where δ is the isotopic enrichment of ^2H and ^{18}O relative to SMOW. Local deviations from the GMWL can occur. In areas with low relative humidity, the slope of the meteoric water line decreases due to partial evaporation of water droplets falling in the sky, so it is helpful to develop of Local Meteoric Water Line (LMWL), when available (Gat, 2010).

Meteoric waters tend to show greater depletions of heavy isotopes at higher latitudes as Rayleigh fractionation occurs and vapor is removed from poleward-moving air (Craig, 1961). Rayleigh fractionation can be described by equation 3 (Faure and Mensing, 2005). In addition, waters show greater depletion at high elevations and at locations farther inland due to the previous removal of vapor (Gat, 2010).

$$R_v = R_v^0 f^{\alpha-1}$$

Equation 3

Where R_v is the isotope ratio of water vapor remaining in an air mass in which condensation is occurring, R_v^0 is the isotope ratio in the air mass before any condensation has occurred, f is the fraction of vapor remaining in the air mass, and α is the fractionation factor, defined by the isotope ratio of the liquid divided by the isotope ratio of vapor.

Because the isotopic composition of precipitation is based on temperature and original vapor source, the isotopic composition of rain changes over the season. Throughout the summer, rain becomes more enriched in the heavier isotopes of oxygen and hydrogen (^2H and ^{18}O) due to an enriched vapor source, higher condensation temperatures, and higher rates of evaporation during rainfall (Ingraham, 1998). As a result, it may not be appropriate to use a mean value for the isotopic composition of rain over a season. Just as the isotopic composition of precipitation can change over time, the isotopic composition of snowmelt can change over time. Hydrograph

separations usually use an average value of $\delta^{18}\text{O}$, but the $\delta^{18}\text{O}$ value of snowmelt may differ from the $\delta^{18}\text{O}$ value of the snowpack (Hermann and Stichler, 1981; Taylor et al., 2001). At equilibrium, the $\delta^{18}\text{O}$ enrichment of water is lower than ice, so as snowmelt percolates through the snowpack and reaches equilibrium, the snowpack becomes more enriched in ^{18}O . As snowmelt progresses, the ^{18}O enrichment of snowmelt increases by 1-4‰ (Feng et al., 2002). This evolution should be considered in hydrograph separations using isotopic tracers when possible.

When there are $n+1$ different sources, fully constrained hydrograph separations can usually be performed with n isotope system tracers using equations 4 and 5 (Phillips and Gregg, 2003).

$$\delta_{mixture} = f_A\delta_A + f_B\delta_B + \dots + f_{n+1}\delta_{n+1} \quad \text{Equation 4}$$

$$f_A + f_B + \dots + f_{n+1} = 1 \quad \text{Equation 5}$$

Stable Isotope Analysis in R (SIAR) uses information on the distribution of source isotope composition to determine feasible contribution proportions to a target (Parnell and Jackson, 2015). It fits a Bayesian model based upon a Gaussian distribution, and the output is based upon 95%, 75%, and 50% Bayesian credibility models (Parnell and Jackson, 2015). It was created originally to determine the composition of organisms' diets, but has been used in other stable isotope applications, such as hydrology (Menger, 2015). Stable isotopes, therefore, can provide information about the contribution of different sources to streamflow in beetle-killed watersheds.

The application of stable isotope hydrology to investigating the hydrologic effects of the mountain pine beetle infestation may be helpful in understanding the streamflow mechanisms involved. Stable isotopes were used for source partitioning in the Western Slope of the Rocky Mountains in Colorado (Maggart, 2014; Menger, 2015) (Figure 1). Instead of using end member mixing analysis, these studies employed mixing models such as IsoSource (Phillips and Gregg, 2003) and SIAR (Parnell and Jackson, 2015) to construct feasible ranges of relative source contribution. No significant correlation between beetle kill and relative source contribution was found using ^2H and ^{18}O (Maggart, 2014; Menger, 2015) (Figure 1).

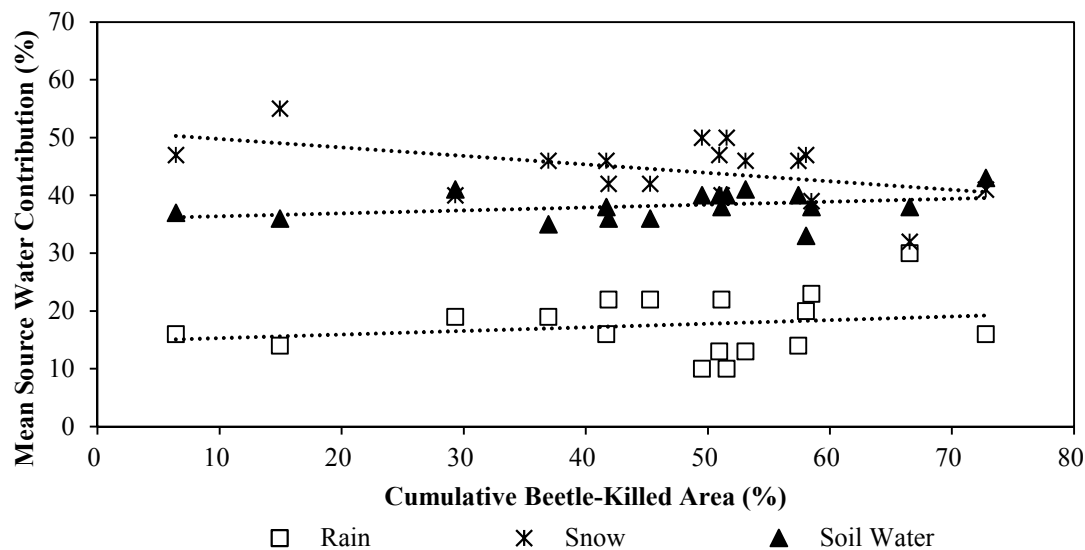


Figure 1. Mean source water contribution vs. cumulative beetle-killed area for 17 watersheds in Grand, Eagle, and Summit County, Colorado (from Menger, 2015).

Chemical Hydrograph Separation

In addition to the use of stable isotopes in mixing analysis, chemical hydrograph separation can provide useful information about changes in source contribution mechanisms in beetle-killed watersheds. Traditionally, hydrograph separations have been limited to graphical approaches. While the widespread availability of discharge data is an advantage for graphical approaches, chemical hydrograph separations can provide more precise, reliable estimations of the contribution of different sources of water to streamflow (Miller et al., 2014). In fact, chemical hydrograph separations sometimes produce more reliable results than environmental isotopes due to temporal variability in isotopic compositions or indistinguishability in isotopic composition between sources (Hooper and Shoemaker, 1986). There are limited studies using hydrograph separation techniques to examine the effects of bark beetle infestation on hydrology (Bearup et al., 2014). However, existing research on event-based hydrograph separation in beetle-killed watersheds suggests increases in surface and subsurface flow, indicating both increased contribution from precipitation and groundwater at the event-scale in beetle-infested watersheds (Beudert et al., 2007). Therefore, hydrograph separation techniques may be useful tools for understanding the hydrologic effects of bark beetle infestation in snowmelt-dominated watersheds. Effective hydrologic tracers should be easily measured and conservative so that conclusions may be drawn about the composition of stream water using mixing equations.

Specific Conductivity

Specific conductivity may be the most effective single parameter to perform a chemical hydrograph separation (Caissie et al., 1996). Specific conductance is a measurement of a solution's ability to conduct an electrical current (Cox et al., 2007). Many studies have employed ionic concentrations and specific conductivity exclusively in order to differentiate streamflow sources (Kunkle, 1965; Nakamura, 1971; Zeman and Slaymaker, 1975; Miller et al., 2014).

Specific conductivity (SC) displays an inverse relation with discharge (Caissie et al., 1996). The specific conductivity of water reveals the extent of that water's interaction with soil (Kronholm and Capel, 2015). Precipitation in Colorado usually has a specific conductivity of less than 10 uS/cm (<http://nadp.isws.illinois.edu/data/ntn/>). As the length of a water source's interaction with the soil increases, specific conductivity increases, so groundwater has a distinctively higher conductivity than surface runoff and direct precipitation (Pilgrim et al., 1979; Winter et al., 1998). A typical value of SC for groundwater is approximately 500 uS/cm, while surface waters with little influence from groundwater show values of approximately 100 uS/cm (Hem, 1985). In snowmelt-dominated watersheds, the stream specific conductivity will increase over time as snowmelt slows and streamflow is predominately composed of groundwater.

Specific conductivity is easily measured *in-situ*, which makes it feasible for most studies. Specific conductivity has been used to determine groundwater discharge during flood events and to verify hydrometric measurements to compute groundwater discharge to a stream during base flow (Kunkle, 1965). Over a large temporal and spatial scale, baseflow contribution in snowmelt-dominated streams was estimated using continuous specific conductivity and discharge data (Miller et al., 2014). The study used two end members (runoff and baseflow), which may be appropriate in larger watersheds. The runoff end member was taken to be 33 uS/cm and the baseflow end member was taken to be the in-stream SC value during low-flow due to variability in groundwater SC values. In the Upper Colorado River Basin, baseflow was found to contribute to 13-45% of discharge during the snowmelt period and 40-86% of discharge during low flow period (Miller et al., 2014). Specific conductivity along with discharge measurements, in this case, proved to be an effective tool to describe streamflow generation mechanisms.

Chloride

Chloride can also be used as a conservative tracer in hydrograph separations. Many studies have used chloride to attempt hydrograph separations for stormflow (Rice and Hornberger, 1988; Caissie et al., 1996; Munyaneza et al., 2012). “New” water, or stormflow, can be separated from “old” water, or groundwater using chloride measurements (Peters and Radcliffe, 1998). However, fewer studies have been conducted using chloride to separate streamflow sources in snowmelt-dominated watersheds over longer periods of time (Liu et al., 2004). In addition, no studies have used chloride to conduct hydrograph separations in beetle-killed watersheds. However, chloride may provide a useful tool, in combination with specific conductivity, to determine source contributions in beetle-killed watersheds. Chloride is a mobile anion and does not participate in many common geochemical reactions, which makes it ideal for use as a conservative tracer (Hem, 1985). Specific conductivity may provide a simple method for hydrograph separation, but results can be verified by other conservative tracers, such as chloride (Covino and McGlynn, 2007).

For source separations with chloride to be successful, each source must have discernably different concentrations. In addition, chloride levels must be high enough to exceed the minimum detection limit of the equipment, which is not always the case (Caissie et al., 1996). In addition, the sample from each source must be representative of the whole source, which may present a problem when hyporheic exchange brings about direct exchange between surface and groundwater. When there are more than two possible sources to streamflow, combining hydrologic tracers can be helpful in determining relative source contribution.

End Member Mixing Analysis (EMMA)

In some cases, it may be helpful to combine tracers (like chloride and specific conductivity) in order to quantify source contributions to streamflow. Many source separation studies use end member mixing analysis (EMMA) to quantify the contribution of different sources to stream flow (Hooper and Shoemaker, 1986; Liu et al., 2004; Kronholm and Capel, 2015).

$$Q_s * C_s = Q_1 * C_1 + Q_2 * C_2 + Q_3 * C_3 \dots + Q_n * C_n \quad \text{Equation 6}$$

$$Q_s = Q_1 + Q_2 + Q_3 \dots + Q_n \quad \text{Equation 7}$$

Where Q_s is stream discharge, C_s is in-stream concentration, and Q_n , and C_n represent the water contribution and concentration from each end member, or source. EMMA requires continuous discharge measurements, concentration of one or more constituents (Kronholm and Capel, 2015), and can be conducted using equations 6 and 7 (Hooper and Shoemaker, 1986). EMMA includes the identification of conservative tracers and possible end members through principal component analysis (Liu et al., 2004). Principal component analysis involves the determination of which tracers account for the most variation, or those that are not highly correlated, and these are used in EMMA (Christopherson and Hooper, 1992). End member mixing analysis, complete with principal component analysis, can provide a better estimation of true source contribution to streamflow than simply randomly choosing conservative tracers (Liu et al., 2004). Streamflow values of tracers should fall between source tracer concentrations, as it represents a mix of sources (Liu et al., 2004). EMMA requires the use of $n-1$ tracers, where n is the number of possible end members included in the analysis. EMMA also requires discernable differences in source chemical composition in order to produce reliable results as compared to graphical approaches (Kronholm and Capel, 2015).

In two small watersheds in Rocky Mountain National Park, ^{18}O and electrical conductivity were used to perform a three-component hydrograph separation (Bearup et al., 2014). The two watersheds exhibited different levels and stages of mountain pine beetle infestation. Using a paired watershed approach, it was found that greater fractions of groundwater contribute to streamflow after infestation and in watersheds with larger areas affected by MPB (Bearup et al., 2014). This increase is attributed to transpiration loss and decreased SWE in MPB-affected watersheds.

Hypothesis and Study Objectives:

It was hypothesized that hydrologic changes associated with the mountain pine beetle kill have changed streamflow generation mechanisms (SGM), and that these changes are measureable using isotopic and chemical tracers. Specific objectives were to determine if SGM under beetle-killed forests can be separated using:

1. ^2H and ^{18}O isotopes of source waters.
2. Specific conductivity of source waters and a two-component hydrograph separation method.
3. Chloride concentration of source waters and a two-component hydrograph separation method.
4. Chloride and specific conductivity in EMMA.

METHODS

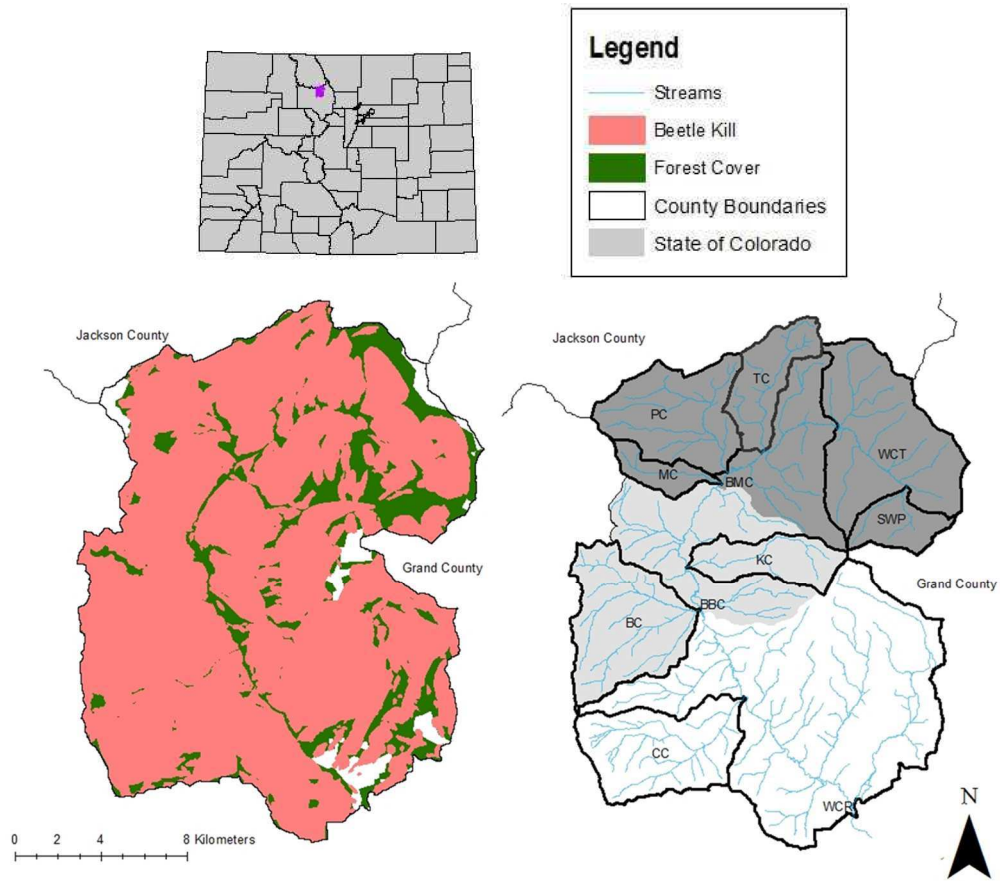
Site Description:

This study was conducted over the 2015 water year, using 11 subwatersheds of the Willow Creek upstream of Willow Creek Reservoir, Grand County, CO (Figure 2). This area is dominantly lodgepole pine forests with varying degrees of bark beetle infestation (Figure 2). The watershed area consists mostly of United States Forest Service land, with little development in the area, aside from off highway vehicle (OHV) activity. These sites were chosen due the area of beetle kill (Table 1) and site access. The watersheds are nested and enter Willow Creek Reservoir (WCR) (Figure 2). The annual hydrograph for these watersheds is snowmelt dominated, with peak flows resulting from spring snowmelt. Between 2005 and 2015, peak flows ranged from 11-47 m³/s at WCR (northernwater.org).

A Geographic Information System (GIS) was used to calculate watershed area, elevation, forest layers, and MPB kill layers. Elevation was obtained from a 10-meter resolution digital elevation model (USGS, 2013). The mountain pine beetle kill layer for 2002 to 2014 was obtained by the USFS Aerial Detection survey (USDA, 2014), and the forests layer was obtained from the 2005 National Land Cover Data set (USGS, 2005).

Table 1. Watershed names, site ID, watershed area, average elevation, and percent of total watershed area affected by the mountain pine beetle for each site.

Site	Site ID	Area (km ²)	Average Elevation (m)	Beetle Kill (%)	Forested Area (%)
Stillwater Pass	SWP	8.4	3148	47.1	98.2
Willow Creek above Trout	WCT	47	3100	64.4	95.3
Trout Creek	TC	13.5	2931	91	100
Pass Creek	PC	24.9	2985	87	93.5
Mulstay Creek	MC	5.8	3048	97.3	96.3
Willow Creek below Mulstay Creek	BMC	115.8	3012	77.8	96.3
Kauffman Creek	KC	12.8	3013	89.1	91.6
Buffalo Creek	BC	29.6	2841	97.4	100
Willow Creek below Buffalo Creek	BBC	192.7	2957	83.7	97.2
Cabin Creek	CC	27.3	2956	93.3	100
Willow Creek above Reservoir	WCR	325.9	2919	86.1	96



Projection: UTM Zone 17 NAD 1983

Data Source: USGS and NRCS

Date: 06 March 2016

Figure 2. Watershed location (above), site locations (right), and beetle kill extent (left) in Willow Creek Watershed, Grand County, CO.

Isotopy

Field Procedures

Surface, groundwater, and precipitation samples were taken between April and October 2015, approximately semi-monthly (Table A-1). For surface water samples, 20 mL polypropylene scintillation bottles were submerged and capped under water to avoid air bubbles. Ground water samples were obtained using PVC or stainless steel piezometers and a vacuum pump. Piezometers were shallow (<1 m deep) and located in the riparian zone. The twenty mL polypropylene scintillation bottles were filled for isotope analysis and capped tightly to prevent air entrapment, which can lead to fractionation.

Precipitation (rain and snow) samples were taken at Willow Creek Pass near the SnoTel station (869). Previous work revealed that the isotopic compositions of precipitation do not vary spatially in this region (Maggart, 2014). The snow sample was collected in a plastic bag and allowed to melt before filling the sample bottle. Rain samples were collected using the International Atomic Energy Agency precipitation sampler of a brown one-liter polypropylene bottle, sawing the top off, and placing it one meter above ground level (IAEA, 1997). A layer of paraffin oil was used to prevent evaporation and isotopic enrichment of the precipitation sample. The paraffin oil was allowed to separate from the sample in the lab. The 20 mL samples of groundwater, surface water, and precipitation were analyzed at the University of Wyoming Stable Isotope Facility (UWYSIF, 2015).

Data Analysis

Stable Isotope Analysis in R (SIAR) requires isotopic data of a target and its sources and fits a Bayesian model to potential sources based on a Gaussian likelihood (Parnell and Jackson, 2015). The model requires an input of streamflow isotope composition for each sample date and mean and standard deviations of source isotope compositions. The model then runs a Markov Chain Monte Carlo (MCMC) simulation with a dirichlet prior distribution on the mean. SIAR was run separately for each study watershed, using the site's streamflow compositions as a target file and rain, snow, and site groundwater data as source files. Due to the small sample size rain (n=5) and snow (n=1) collected, precipitation isotope data from 2011-2012 in the region supplemented the 2015 data (Maggart, 2014). These precipitation data were used to create a local meteoric water line (LMWL). Groundwater and surface water samples were plotted along with this line to observe trends.

In order to determine whether the groundwater and surface water samples were sufficiently different in isotopic composition, a two-tailed t-test for differences between the means was performed. Mean surface water was subtracted from mean groundwater at each site, and a p-value for $H_0: \mu_{\text{groundwater}} = \mu_{\text{stream}}$ was calculated.

Mean source contributions throughout the sampling period were determined using mean values for rain and groundwater. The target file includes all isotope measurements of the stream water (for both ^2H and ^{18}O), while the source file includes the mean and standard error of each source isotope composition (for both ^2H and ^{18}O). Default settings on the program were used, with 500,000 iterations and the first 50,000 were discarded (Inger et al., nd). The output of the model includes intervals of 50%, 75%, and 95% Bayesian credibility standards for relative contribution of each source.

These relative contributions of each source were plotted for each watershed against % area of beetle kill. Statistical significance of this line was assessed using Spearman's rank order correlation. Spearman correlation differs from the traditional Pearson correlation because the correlation coefficient, ρ , is 1 when the two variables are monotonically related, even if the relation is not linear. Spearman's rank order coefficient, ρ , is calculated using equation 8 (McDonald, 2014). The variables are first ranked in descending order and then assigned a rank (x_i, y_i) based on the ordinal position.

$$\rho = \frac{\sum_i(x_i - \bar{x})(y_i - \bar{y})}{\sqrt{\sum_i(x_i - \bar{x})^2 \sum_i(y_i - \bar{y})^2}} \quad \text{Equation 8}$$

Statistical significance, the p-value, of the correlation coefficient is determined by Student's t-distribution.

The relative contribution of each source was also determined at different sampling dates for the downstream site (WCR). Due to wide seasonal variation in rain isotope composition, a relative contribution was determined for each day a rain sample was taken. The target file included the stream isotope composition for that day; while the source file included the snow isotope composition sampled on April 18, 2015, mean groundwater isotope composition for the season, and the rain sample corresponding to that day.

Chemical Hydrograph Separation

Specific Conductivity

Field Procedures

Surface water and groundwater specific conductivity and temperature were measured *in-situ* using a SPER Scientific® 840039 temperature-correcting conductivity meter. Snow specific conductivity was measured in the lab after melting. Rain specific conductivity was measured in the lab after separating the sample from paraffin oil.

Data Analysis

Groundwater and surface water specific conductivity values were compiled and plotted for each site over time to visually assess results. In order to determine whether the groundwater and surface water samples were sufficiently different in specific conductivity values, a two-tailed t-test for differences between the means was performed. Mean surface water was subtracted from mean groundwater at each site, and a p-value for $H_0: \mu_{\text{groundwater}} = \mu_{\text{stream}}$ was determined.

Specific conductivity was used in a one-tracer, two-component hydrograph separation to determine relative source contributions to streamflow (Pinder and Jones, 1969; Sklash and Farvolden, 1979). Using the equations (9-10) below, mean fractional groundwater contributions were calculated at each site.

$$SC_{\text{stream}} = f_{\text{precipitation}} * SC_{\text{precipitation}} + f_{\text{gw}} * SC_{\text{gw}} \quad \text{Equation 9}$$

$$1 = f_{\text{precipitation}} + f_{\text{gw}} \quad \text{Equation 10}$$

Where SC is the specific conductivity and f is the fractional contribution of each source (groundwater and precipitation). Mean source contribution was analyzed for correlation with beetle kill area using Spearman's rank order correlation (Wessa, 2015). In addition, fractional contribution of groundwater was determined at each sampling date. The results were plotted over time at each site to assess temporal patterns of streamflow generation.

Chloride

Field Procedures

Each 125 mL polypropylene sample bottle intended for chloride measurements of surface water was triple-rinsed before filling. Due to small values of groundwater in the piezometers, clean 100 mL polypropylene bottles

were filled directly with groundwater and stored in a cooler. Snow samples were collected in Ziploc® plastic bags and allowed to melt before being measured for chloride. Rain samples were allowed to separate from paraffin oil before being assessed for chloride.

Lab Procedures

Chloride was measured in the laboratory using a Hach sensION+ 9652 Chloride Ion Specific Electrode® (ISE). 25 mL samples were mixed with a chloride ionic strength adjuster to minimize interference with other ions and placed on a stir plate. Using an Orion® model 290A meter and a set of chloride standards, electrical potential was measured (mV) and related to the negative log of chloride concentration in each sample. A separate calibration curve was generated for each set of samples to account for drift in probe measurements over time.

Data Analysis

Chloride was used in a two-component hydrograph separation to determine relative source contributions to streamflow (Pinder and Jones, 1969; Sklash and Farvolden, 1979). In order to determine whether the groundwater and surface water samples displayed significantly different chloride concentrations, a two-tailed t-test for differences between the means was performed. Using the equations (11-12) below and chloride values, relative source contributions were assessed for each sampling date. Precipitation sample concentrations were obtained from NADP chloride measurements at Buffalo Pass (NTN site: CO 97) (NADP, 2015).

$$Cl^-_{stream} = f_{precipitation} * Cl^-_{precipitation} + f_{gw} * Cl^-_{gw} \quad \text{Equation 11}$$

$$1 = f_{precipitation} + f_{gw} \quad \text{Equation 12}$$

Mean source contribution was analyzed for correlation with beetle kill area using Spearman’s rank order correlation (Wessa, 2015).

Because both chloride and isotopic (²H and ¹⁸O) enrichment are evaporation-driven processes, the results of these methods were compared. Fractional groundwater contribution using isotopy was plotted against fractional groundwater contribution using chloride and assessed for correlation using Spearman’s rank order correlation.

Temporal patterns in groundwater contribution were also assessed using this method. Fractional contribution was determined for each sampling date at WCR, and values were plotted over time with discharge.

End Member Mixing Analysis (EMMA)

Chloride and specific conductivity measurements were combined to determine the relative contribution of each source to streamflow. Mixing diagrams were created, in order to assess if the three source values formed bounds around streamflow values (Liu et al., 2004). Specific conductivity was plotted vs. chloride concentrations for each source and streamflow, and the plots were assessed for compliance.

Relative contribution of groundwater to streamflow was determined using a three-component, two-tracer analysis (Equations 6 and 7). Mean source contribution was analyzed for correlation with beetle kill area using Spearman's rank order correlation (Wessa, 2015).

Because this method employs specific conductivity and chloride as tracers, the results of fractional groundwater contribution using specific conductivity and chloride as a tracer were assessed for correlation using Spearman's rank order correlation to determine agreement between the two methods. Finally, temporal patterns of fractional groundwater contribution were assessed at the downstream site, WCR by using the mixing equations at each date.

RESULTS AND DISCUSSION

Isotopy

Isotope composition results from the University of Wyoming Stable Isotope Facility are accurate to 0.2‰ for ^{18}O measurements and 1‰ for ^2H measurements (UWSIF, 2015). A local meteoric water line (LMWL) was created using precipitation from the Colorado Rocky Mountains from 2011-2015 and fitting a line ($\delta^2\text{H} = 7.9 * \delta^{18}\text{O} + 8.9$) to the data (adapted from Menger, 2015). This line differs slightly from the GMWL (Equation 2). Measurements of isotopic signature in source waters (groundwater, rain, and snow) showed distinct separation along the LMWL (Figure 3a). Isotopic composition of rain and snow are variable based on condensation temperature (Ingraham, 1998). Snow measurements were depleted relative to rain and groundwater in ^2H and ^{18}O , while rainwaters were less depleted relative to groundwater and snow, which is consistent with the formation temperature of each species. Because snow condenses at a lower temperature, it is depleted in heavy isotopes relative to rain.

Precipitation samples fall along the LMWL (Figure 3a). Evaporation brings about enrichment in heavier isotopes of hydrogen and oxygen, as the lighter isotopes evaporate more readily. In addition, preferential evaporation of ^2H in subsurface water brings about depletion in ^2H , relative to ^{18}O , or a lower *d-excess* value (Gat, 2010). As a result, most of the groundwater and surface water samples fall below the LMWL, with a lower slope, indicating evaporation (Figure 3b).

A mixing model, Stable Isotopes in R (SIAR), was used to determine the fractional contributions of source waters to streamflow. In order to use mixing equations effectively, each source should have distinct tracer compositions from each other and from the surface water (Sklash and Farvolden, 1979). In this case, groundwater and surface water samples showed similar isotopic composition, so they were plotted with the LMWL to visually assess differences between isotopic signatures (Figure 3b). Groundwater and surface water samples occupy the same range. The most depleted values are surface water samples, while the most enriched values are groundwater samples. A two-tailed t-test was performed to determine whether the groundwater and surface water samples were significantly different. A two-tailed t-test was used to test for differences between means ($H_0: \mu_{\text{sw}} \neq \mu_{\text{gw}}$). Mean surface water and groundwater stable isotope composition were found to be significantly different ($\alpha=0.10$) at WCR

and CC, but not at any other site (Table 2). Groundwater and surface water isotopic compositions may not be sufficiently different for mixing analysis at other watersheds.

Mean contribution of each source water to each of the 5 sampled watersheds over the season were determined using mean and standard deviations of the source waters and streamflow. Results were then plotted against beetle-killed forest area and Spearman rank order correlation (ρ) determined (Figure 4). Rain was the smallest contributor to streamflow, and groundwater was the largest contributor over the sampling period. Groundwater was positively correlated with increasing beetle-killed forest area ($p=0.23$), indicating increasing groundwater contribution to streamflow with the mountain pine beetle kill. Rain and snow contribution were negatively correlated with beetle-killed forest area ($p=0.08$ and $p=0.35$ respectively), indicating decreasing precipitation contribution to streamflow with the mountain pine beetle kill (Figure 4).

Mean precipitation isotope composition was used for mixing analysis; however, precipitation isotope composition varies with formation temperature. As the temperature becomes warmer, precipitation becomes less depleted in heavy isotopes (^2H and ^{18}O). Thus, in addition to assessing the mean contribution of each source, source contribution at each sampling date was assessed (Figure 5). Precipitation data from WY 2015 were used to assess temporal patterns. SIAR was run separately using these data for each sample date, using stream and rain isotopic composition from that sample date at the downstream site, WCR (Figure 5). Snow increased in fractional contribution, even after the cessation of snowmelt, while rain decreased in fractional contribution. However, all the snow had melted by June 3, 2015 (Figure 6), so the attribution of snow may be an artifact of the mixing model. Because rain becomes increasingly enriched and the groundwater signature is similar to the stream water, a portion of the streamflow is assigned to snow.

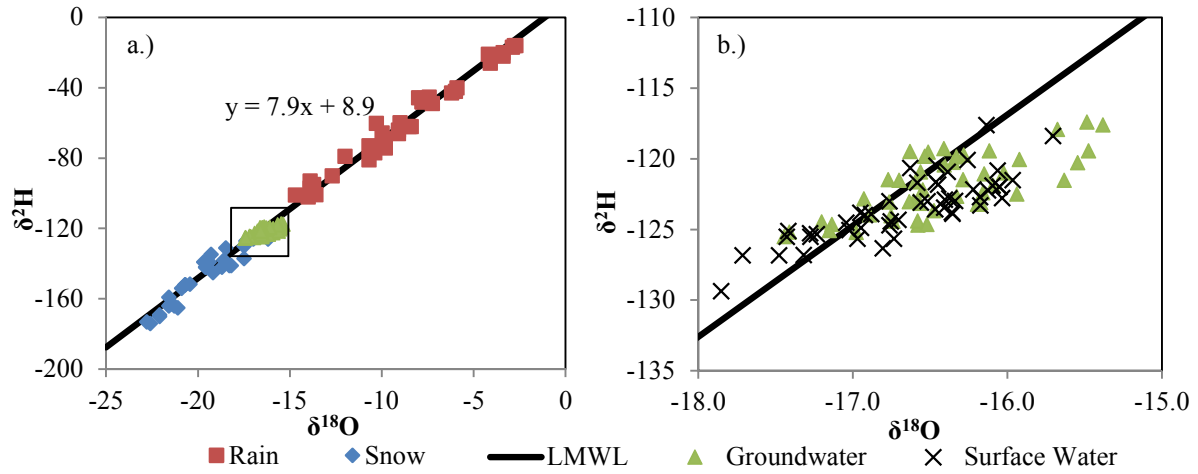


Figure 3. Isotopic composition of source waters (a) including precipitation data collected from 2011 to 2015 with a LMWL for the Colorado Rocky Mountains (Menger, 2015) and b.) groundwater and surface water isotope compositions for all of the sites during water year 2015, plotted with the LMWL (Menger, 2015).

Table 2. Difference between mean groundwater and surface water isotope compositions and associated two-tailed p-values.

Site	δ ² H		δ ¹⁸ O	
	GW - SW (‰)	p-value	GW - SW (‰)	p-value
WCR	2	0.01	0.3	0.06
BC	0	0.62	0.1	0.57
WCT	1	0.27	0.1	0.55
SWP	3	0.15	0.4	0.14
CC	2	<0.01	0.3	0.04

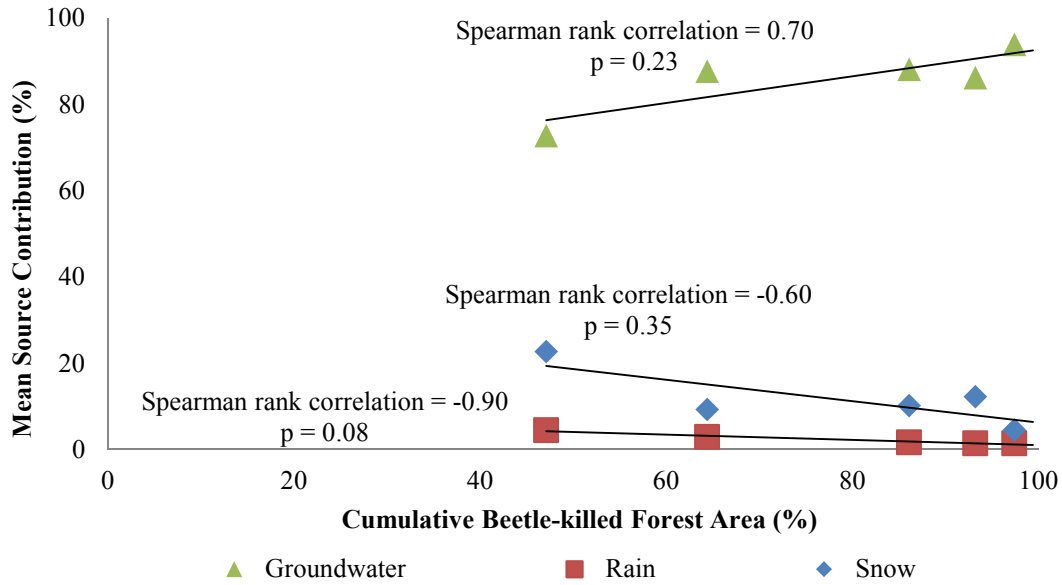


Figure 4. Average rain, snow, and groundwater contribution to streamflow vs. beetle-killed forest area (%) for 5 subwatersheds in Willow Creek watershed from April-October 2015.

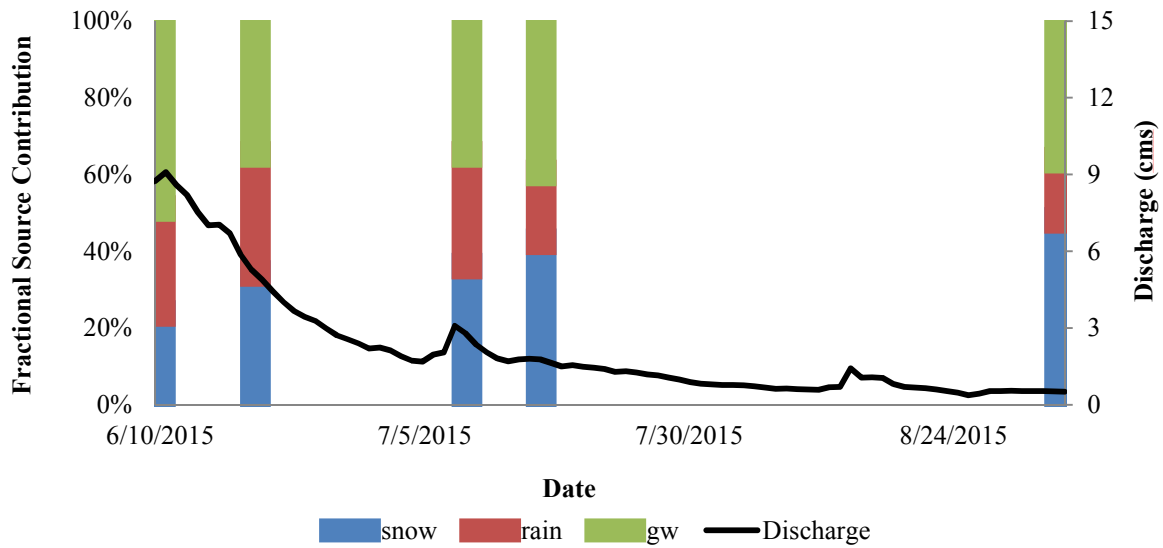


Figure 5. Rain, snow, and groundwater contribution to streamflow at Willow Creek above Reservoir (WCR) over the sampling season.

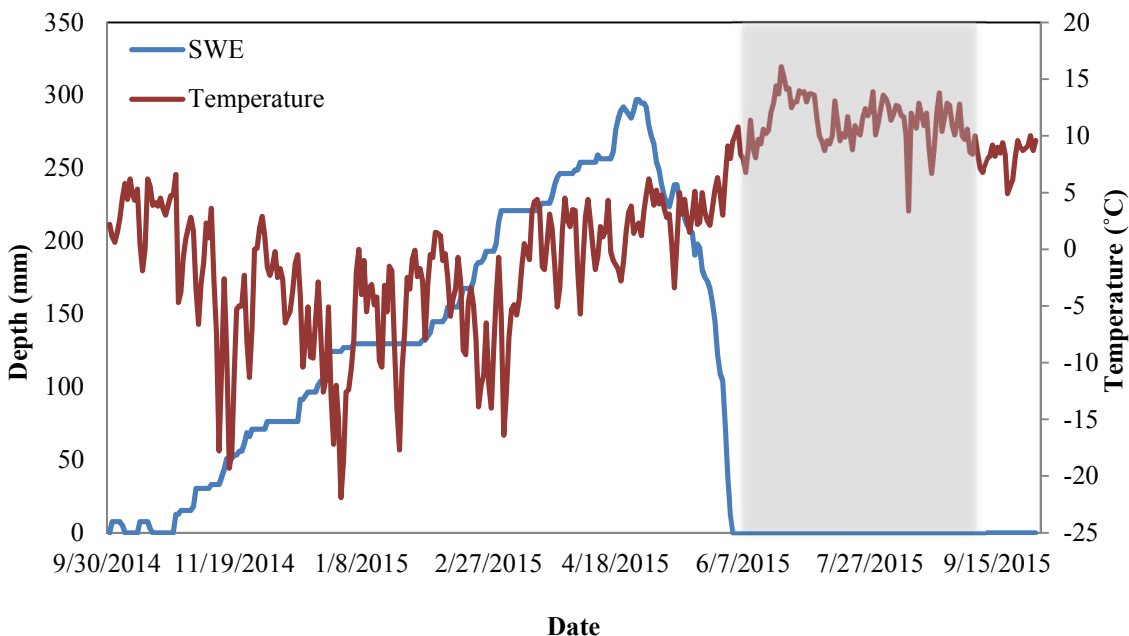


Figure 6. Snow water equivalent, temperature, and precipitation over the 2015 water year. SnoTEL site 869 historical daily data (NRCS, 2015). Temperature data from GRAND LAKE 6 SSW station (<http://www.ncdc.noaa.gov/>). The extent of Figure 5 is shown in grey.

SGM waters had distinct isotopic compositions, but precipitation isotope compositions were variable. Stable isotope fractionation in precipitation is formation temperature dependent, so stable isotope compositions of rain and snow vary seasonally (Ingraham, 1998). A local meteoric water line (LMWL) was used for comparison to groundwater samples (Menger, 2015) because groundwater isotopic signatures are enriched compared with meteoric water due to preferential evaporation of lighter isotopes (Ingraham, 1998). Evaporation of meteoric water leads to lower values and slopes than the meteoric water line (Gat, 2010) (Figure 3b). As a result, most of the groundwater samples fall below the LMWL and exhibit a smaller slope.

Isotope composition of source waters and stream water were used in into Stable Isotope Analysis in R (SIAR) in order to determine a range of probable contribution from each source. Using Spearman's rank order correlation, rain contributions were negatively correlated with beetle-killed forest area ($p=0.08$) (Figure 4). Snow was negatively correlated with beetle-killed forest area ($p=0.35$), and groundwater was positively correlated with beetle-killed forest area ($p=0.23$) and suggests that groundwater contribution increases with increasing beetle-killed forest area.

Conducting a study in nested watersheds minimizes spatial variability of precipitation volume and composition. While precipitation will still exhibit spatial variability, it is minimized by decreasing the spatial extent

of the study. It should be noted, however that redundancy is inherent in nested watershed studies. The effect of beetle kill is, in effect, double counted when nested watersheds are included in the study. For example, the site BMC includes the site WCT, which includes SWP. This may lead to an increased likelihood of detecting statistically significant correlations.

Early studies on the effect of bark beetle infestation on streamflow indicated increases in annual water yield following infestation (Love, 1955; Bethlahmy, 1974; Potts, 1984). Streamflow models also predict an increase in groundwater contribution to streamflow, driven by the cessation of transpiration in killed trees (Pugh and Gordon, 2013). Recently, a paired watershed study using specific conductivity and ^{18}O as tracers also detected an increase in groundwater contribution to streams corresponding with the onset of beetle-kill (Bearup et al., 2014). However, recent works support the finding that there is no significant correlation between beetle-killed forest area and fractional source contribution (Maggart, 2014; Menger, 2015). In addition, recent models indicate no relationship between bark beetle infestation and increased water yield due to increased surface evaporative losses (Biederman et al., 2014; Biederman et al., 2015).

Average source contribution over the entire watershed (using the downstream site, WCR), indicates an average source contribution of 88% groundwater, 2% rain, and 10% snow. These values differ considerably from previous work in the region of 38% groundwater, 18% rain, and 44% snow (Menger, 2015) and 20% groundwater, 20% rain, and 60% snow (Maggart, 2014) (Table 3). This study sampled frequently from April to October 2015, while previous studies sampled year-round (Maggart, 2014; Menger, 2015), which would lead to higher groundwater contribution from frequent baseflow sampling. In addition, the studies did not use the same mixing model. IsoSource, which does not account for the propagation of error throughout the mixing model, was used in the first study (Maggart, 2014). When the data were resampled using measurements for the same watershed, the same months of the year, and the same mixing model, groundwater contribution increased, but was still considerably lower than the values observed in this study (Table 4). 2015 was a below average snowpack year, which could further explain the smaller relative contribution of snow to streamflow, and the study sites display a higher degree of beetle kill compared to previous work.

Table 3. Mean source water contributions for each study conducted using stable isotopes (2H and 18O) in the Rocky Mountains of North-Central Colorado.

Study	Program Used	Groundwater	Rain	Snow
Maggart (2014)	IsoSource	20%	50%	60%
Menger (2015)	SIAR	38%	18%	44%
Wehner (2016)	SIAR	88%	2%	10%

Table 4. Source water contributions for each study period at Willow Creek above the Reservoir (WCR), resampled for dates between April and October and re-analyzed using SIAR.

Source	Sampling Period	Sampling Dates	Groundwater	Rain	Snow
Menger (2014)	4/27/12 - 8/17/12	5	52%	10%	38%
Wehner (2016)	4/28/15 - 10/2/15	11	88%	2%	10%

Alternatively, the high contribution of groundwater may be due to similarities between groundwater and stream water isotopic (Figure 3b, Table 2). The groundwater piezometers were drilled to less than 1 meter depth, and were adjacent to the stream. Colorado mountain streams can display connectivity to subsurface flow paths, resulting in water with surface water signatures flowing through the subsurface (Harvey and Bencala, 1993). If the groundwater samples represented a hyporheic exchange, they would display a mixture of groundwater and surface water characteristics, and an overestimation of groundwater input to streamflow at all sites. If the groundwater samples were, in fact, an accurate representation of groundwater isotope composition, the similarity with surface water composition might be problematic for mixing analysis (Sklash and Farvolden, 1979; Kronholm and Capel, 2015).

To account for the high variability of precipitation isotope compositions, separate mixing equations were performed for each sampling date. Temporal analysis of fractional source contribution using SIAR showed an increase in contribution from snow in the late summer, after the cessation of snowmelt. The date of cessation of snowmelt is likely a conservative estimate, as the data provided is from the SnoTel station (869), located at Willow Creek Pass, which displayed higher snowpack persistence than lower elevations. Throughout the summer, rain becomes enriched in heavy isotopes. However, the groundwater is not depleted in comparison to the surface water samples (Table 2). As a result, SIAR returns a result of increasing snow to compensate. In snowmelt dominated systems, groundwater dominates low flows after the cessation of snowmelt. Poor separation between surface water and groundwater isotope composition may have affected this result. Chemical hydrograph separations can produce more reliable results due to isotopic variability and similarities in composition between source waters (Hooper and Shoemaker, 1986).

Similarities between groundwater and surface water stable isotopic signatures limited the utility of stable isotopes as tracers in this study. It is likely that hyporheic exchange occurred at some sites, and the sampled isotope compositions are not an accurate representation of the true groundwater values. Even if the isotopes are representative of the groundwater signature, mixing equations require discernable differences between each component (Sklash and Farvolden, 1979; Kronholm and Capel, 2015).

Chemical Hydrograph Separation

Specific Conductivity

Specific conductivity of groundwater is higher than that of precipitation or surface water. For a mixing equation to effectively separate sources of streamflow, each source must display distinct tracer concentrations. Specific conductivity values for stream water ranged from 32.1 to 116.2 $\mu\text{S}/\text{cm}$ while values for groundwater ranged from 32.3 to 477 $\mu\text{S}/\text{cm}$. Mean specific conductivity for rain was 15.0 $\mu\text{S}/\text{cm}$ and 2.7 $\mu\text{S}/\text{cm}$ for snow. Mean groundwater and surface water specific conductivities were compared using a two-tailed t-test. In all cases, mean groundwater specific conductivity was greater than surface water specific conductivity, and this difference was significant at 6 of the 11 sites at the $\alpha = 0.05$ level and 8 of the 11 sites at the $\alpha = 0.10$ level (Table 5), suggesting that specific conductivity is an appropriate tracer.

Table 5. Difference between mean groundwater and surface water specific conductivity ($\mu\text{S}/\text{cm}$) and chloride concentration (mg/L) with a two-tailed p-value for each site.

Site	SC ($\mu\text{S}/\text{cm}$)	p-value	Chloride (mg/L)	p-value
BBC	27.9	0.03	0.56	0.02
BC	30.0	<0.01	0.27	0.14
BMC	7.3	0.32	1.43	0.01
CC	17.5	0.06	0.76	0.01
KC	5.9	0.25	0.28	0.11
MC	22.6	<0.01	3.26	<0.01
PC	18.2	0.12	0.41	0.14
SWP	20.2	0.06	0.46	0.29
TC	47.5	<0.01	1.60	<0.01
WCR	100.2	<0.01	2.55	<0.01
WCT	301.2	<0.01	2.28	<0.01

The mean groundwater contribution for each site was plotted against beetle kill area (Figure 7). Spearman's rank order coefficient was used to determine the statistical significance of the relation between beetle kill area and fractional groundwater contribution. Beetle kill was negatively correlated with average groundwater contribution ($\rho = -0.13$), but the result was not significant ($p = 0.71$). These results indicate that streamflow generation mechanisms do not change significantly with increasing beetle-killed forest area, but that groundwater input to streams may decrease.

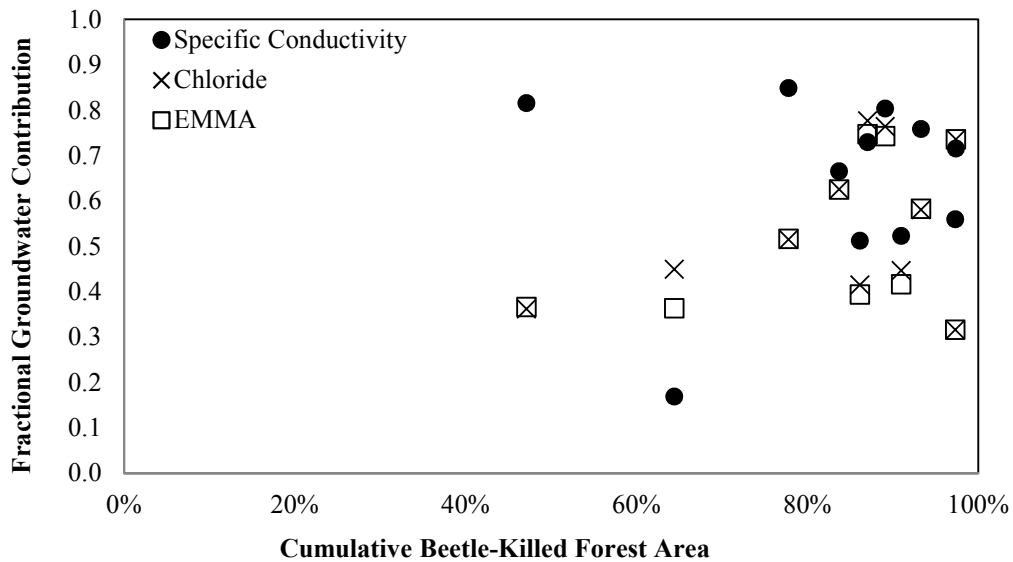


Figure 7. Fractional groundwater contribution vs. beetle kill forest area (%) using specific conductivity ($\rho=-0.13$, $p=0.71$), chloride ($\rho=0.19$, $p=0.58$), and end member mixing analysis ($\rho=0.26$, $p=0.43$).

Specific conductivity was used in a two-component (precipitation and groundwater) mixing equation (Equations 9-10) to determine the fractional contribution of groundwater at WCR (Figure 8) and each watershed for each sampling date (Figure A-3). The average precipitation conductivity was used for the analysis. Some sites (SWP, WCT, TC, BC, BBC, and WCR) showed increases in relative groundwater contribution during the receding limb of the hydrograph, which is expected in a snowmelt-dominated watershed (Figure A-3). However, this may reflect a combination of increasing surface water specific conductivity and decreased groundwater specific conductivity during baseflow (Figure A-2).

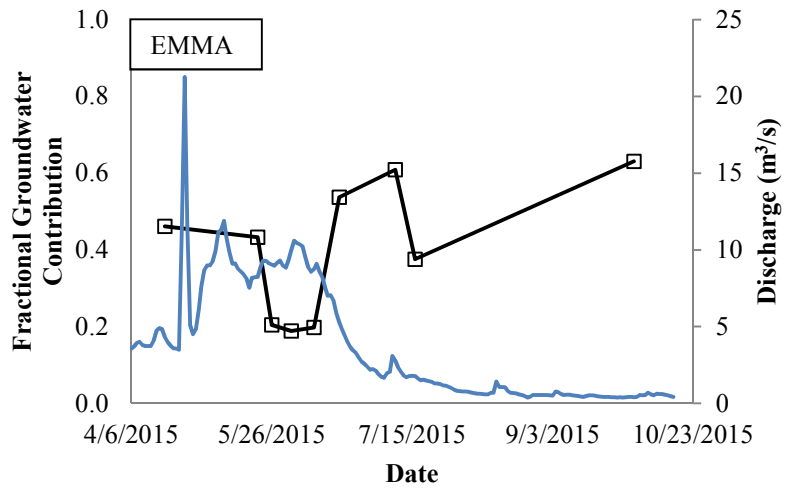
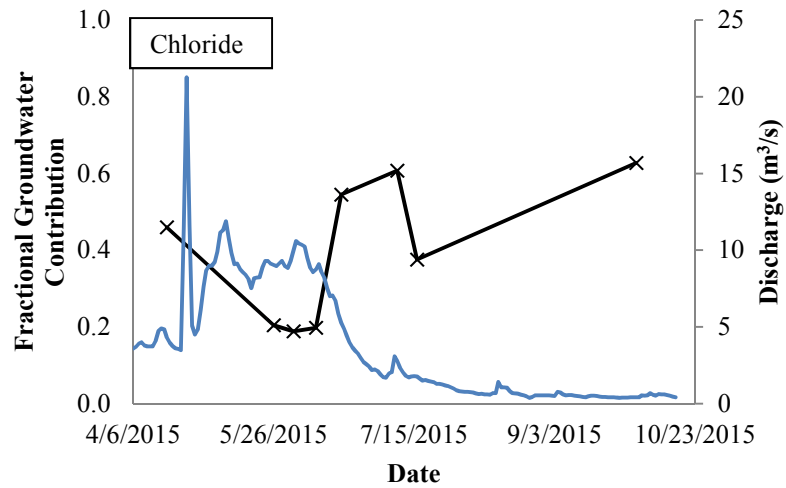
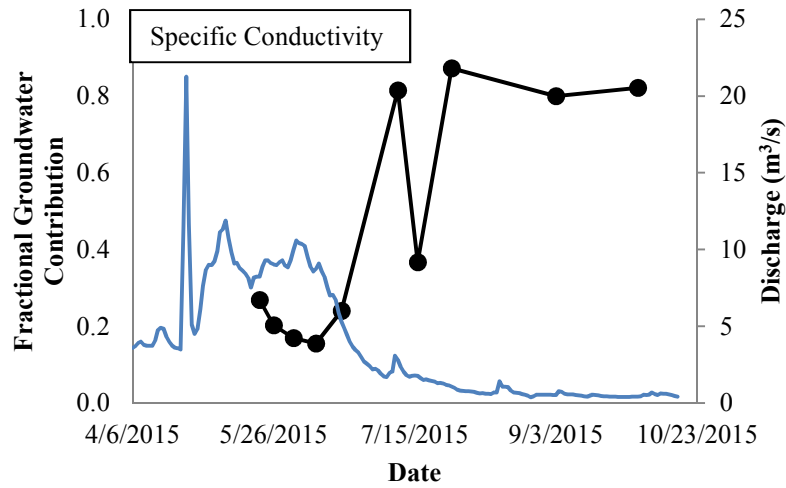


Figure 8. Fractional groundwater contribution and discharge for each sampling date at WCR using each tracer method.

Chloride

Chloride increases in groundwater as a result of evapoconcentration. As a result, groundwater subject to high rates of evaporation tends to exhibit higher chloride concentrations. Stream water chloride concentrations ranged from 0.28 mg/L to 2.21 mg/L, while groundwater chloride concentrations ranged from 0.54 mg/L to 10.01 mg/L (Table A-1). Groundwater concentrations showed high variability, with sharp increases corresponding with the July 8th rain event in WCR, MC, and KC (Figure A-4). Groundwater and surface water chloride concentrations were assessed for differences using a t-test in order to assess suitability for use in a mixing equation. Groundwater concentrations were significantly larger than surface water concentrations at 7 of the 11 sites (Table 5), indicating that chloride is a suitable tracer.

Chloride was used in a two-component (precipitation and groundwater) mixing equation (Equations 11-12) to determine the fractional contribution of groundwater for each site. The average chloride concentration in precipitation over water year 2015 from NADP was used in the analysis (0.04 mg/L). Any instances of groundwater contribution above 100% from the model were excluded from the analysis. These results were positively correlated between fractional groundwater contribution and beetle-killed forest area, which was positively correlated ($\rho=0.19$), indicating increases in groundwater contribution with increasing beetle kill ($p=0.58$) (Figure 7).

Chloride was used in a two-component (precipitation and groundwater) mixing equation (Equations 9-10) to determine the fractional contribution of groundwater at WCR (Figure 8). In some cases, the fractional groundwater contribution exceeded 1 or was less than 0, indicating a failure of the mixing model. This can occur when groundwater chloride concentrations are below surface water concentrations. It is expected in snowmelt-dominated watersheds that groundwater input will increase after the cessation of snowmelt and when streams display baseflow conditions. However, there is no evident temporal pattern in groundwater contribution using chloride as a tracer (Figure 8).

End Member Mixing Analysis (EMMA)

Specific conductivity and chloride of each source were assessed to determine if the sources (rain, snow, and groundwater) formed boundaries around streamflow concentrations (Appendix A-5). When this does not occur, the end member mixing analysis will fail, and fractional source contributions will fall below 0 or exceed 1. Streamflow

values at WCR show separation from groundwater values, but do not form bounds in all cases, as the tracer concentrations of snow and rain are very similar (Figure 9).

Specific conductivity and chloride were coupled to determine the fractional contribution of each end member (rain, snow, and groundwater) to streamflow. Using the mixing equations (6 and 7), fractional contributions of groundwater were calculated for each basin. The average chloride concentration in precipitation over water year 2015 from NADP was used in the analysis. Precipitation occurring between May and October was assumed to be rain (0.04 mg/L Cl⁻) and precipitation between December and April was assumed to be snow (0.04 mg/L Cl⁻). Instances of groundwater contribution above 100% were excluded from this portion of the analysis. Contribution of groundwater and beetle-killed forest area was positively correlated ($\rho=0.26$). Results indicate that groundwater contribution to streamflow may increase in watersheds with higher beetle-killed forest area, but the results are not significant ($p=0.43$) (Figure 7).

Specific conductivity and chloride were used in a two-tracer three-component (rain, snow, and groundwater) mixing equation (Equations 9-10) to determine the fractional contribution of groundwater at WCR (Figure 8) for each sampling date. Average values for precipitation were used in the analysis. Again, if the fractional groundwater contribution exceeded 1 or was less than 0, results were excluded. This can happen when groundwater concentrations (Cl⁻ or SC) are below surface water concentrations. There is no evident temporal pattern in fractional groundwater contribution using this method (Figure 8). However, the results of the end member mixing analysis show very similar results to those of chloride, indicating that chloride is a more influential tracer than specific conductivity in this study.

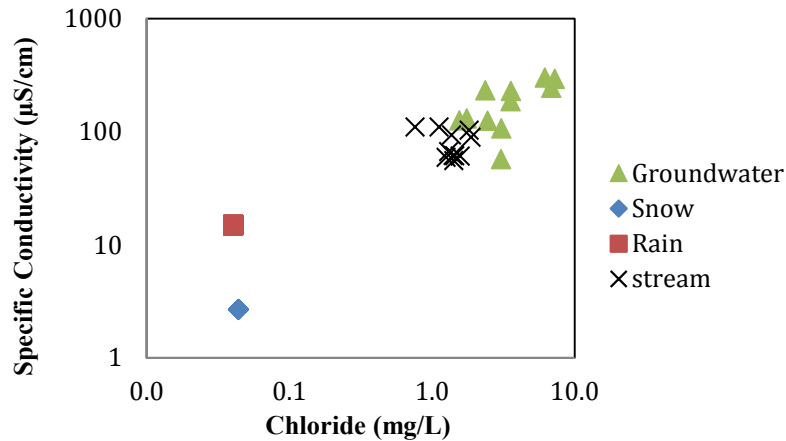


Figure 9. Mixing diagram for WCR including the specific conductivity and chloride concentrations of each source and the stream (shown on a log scale).

Chemical Hydrograph Separation Discussion

Specific Conductivity

Groundwater specific conductivity is higher than that of precipitation or surface water (Pilgrim et al., 1979; Winter et al., 1998). Therefore, it can be used as a tracer for groundwater contribution to streamflow (Miller et al., 2014). Groundwater specific conductivity values were significantly higher ($p < 0.10$) than surface water values for most of the sites (BBC, BC, CC, MC, SWP, TC, WCR, and WCT) (Table 3), suggesting that specific conductivity values may be a valid tracer for hydrograph separation.

A one-tracer two-component mixing equation was used to determine fractional contribution of groundwater to the streamflow, using mean values. These results were assessed for correlation with beetle-killed forest area. Beetle kill was negatively correlated with average ground water contribution ($\rho = -0.13$), but the result was not significant ($p\text{-value} = 0.71$) (Figure 7). These results indicate that beetle-killed forest area is correlated with a decrease groundwater contribution to streamflow, which differs from conceptual models of beetle-induced tree mortality (Pugh and Gordon, 2013). It is possible that the watershed is experiencing increased uptake of groundwater due to revegetation of the understory or that surface evaporation outweighs decreases in transpiration. Alternatively, if the groundwater samples include hyporheic exchange, specific conductivity may be higher due to increased contact with soils, but samples may not accurately represent groundwater specific conductivity for the watershed.

Specific conductivity has been used to quantify groundwater contribution using continuous measurements *in-situ* (Miller et al., 2014). However, the groundwater value for specific conductivity in this case was based on baseflow specific conductivity, not direct groundwater conductivity measurements. Groundwater specific conductivity measurements, especially when located near the riparian zone, can reflect fluctuations in surface water specific conductivity, although the fluctuations are dampened (Cox et al., 2007). Near stream wells can experience interaction with surface waters, causing fluctuations in measured specific conductivity. However, shallow groundwater wells located in the riparian zone can show agreement with deeper, farther wells, depending on degree of hyporheic exchange (Bearup et al., 2014).

Using specific conductivity, fractional groundwater contribution was calculated for each sampling date, using a one-tracer, two-component hydrograph separation. Many sites displayed higher groundwater contribution values at the end of the summer sampling period (Figure 8, Figure A-3), which is consistent with changes from snowmelt-dominated runoff to groundwater-fed baseflow (Miller et al., 2014).

Increases in fractional groundwater contribution may reflect fluctuations in groundwater specific conductivity more than changes in surface water specific conductivity. In most cases, groundwater specific conductivity decreased with the onset of baseflow (Figure A-3). This may reflect an increase in subsurface stream flow, as water tables dropped, and surface water-groundwater interaction increased. During low flow, nearby groundwater wells can reflect the specific conductivity of sub-surface stream flow (Vogt et al., 2010). Even so, most sites had increasing specific conductivity over the sampling period. While groundwater contribution at the end of the sampling period may be overestimated due to sub-surface stream flow, stream water conductivity increases indicate that groundwater contribution increased over the sampling period.

Chloride

NADP chloride concentrations were used in lieu of the measured precipitation chloride concentrations, due to potential sample contamination. When the precipitation samples were used, over half of the fractional estimates were above 100% or below 0%. While measures were taken to avoid contamination, it is important to note this anomaly, as it may have affected the other chloride samples (stream and groundwater). In order to ensure proper functionality and precision of the chloride ISE probe, the slope of a calibration curve should be considered. It is recommended that an ISE provides a difference of at least 54 to 60 mV per order of magnitude of chloride concentration (e.g. 1 to 10 or 10 to 100) (EPA, 1996). However, the ISE probe used in this study ranged from 36 to

58 mV per order of magnitude of chloride concentration. Lower slopes bring about higher uncertainties in chloride concentration, which could affect results, especially with the low concentrations of chloride observed in this study.

Increased chloride concentration in groundwater results from surface evaporation, as water is taken from the system, but constituents in solution remain. As evaporation progresses, the concentration of groundwater chloride increases from evapoconcentration (Jobbagy and Jackson, 2007; Grimaldi et al., 2009). In all cases, groundwater chloride concentrations were higher than surface water concentrations, and this difference was statistically significant at 7 of the 11 sites (Table 5). Chloride was used in a two-component hydrograph separation, and a positive correlation was found between groundwater contribution and beetle-killed forest area ($\rho = 0.19$, $p = 0.58$).

The change in isotope composition of groundwater also relies on evapoconcentration of heavier isotopes, as lighter isotopes are preferentially evaporated. While it is expected that these two methods would show high correlation, the Spearman rank order correlation was $\rho = 0.60$ with a p-value of 0.35 (Figure A-6). Like the isotopy results, groundwater contribution increases with increasing beetle-killed forest area. However, isotopy produces systematically higher results, which might result from similarities between groundwater and surface water isotopic compositions. It is possible that one of the tracers did not act completely conservatively in the system (Kirchner et al., 2010).

While chloride is a conservative tracer in most systems, low tracer concentrations can limit the efficacy of a hydrograph separation (Pinder and Jones, 1969; Caissie et al., 1996). In addition, hyporheic mixing could inflate results of fractional groundwater contribution (Cox et al., 2007). While chloride can be an effective hydrologic tracer, more reliable results can be expected when tracers are combined (Covino and McGlynn, 2007; Cox et al., 2007).

Using chloride, fractional groundwater contribution was calculated for each sampling date at WCR. After the end of snowmelt, it is expected that groundwater increases in fractional contribution, but WCR displayed no evident temporal pattern (Figure 8). There was no evident increase in surface water chloride concentration at any of the sites (Figure A-4).

End Member Mixing Analysis (EMMA)

A combination of specific conductivity and chloride may provide more reliable results than using a single conservative tracer. In order for EMMA to work properly, source concentrations must form boundaries around

streamflow concentrations. At some sites, streamflow is bounded by sources. In other cases, surface water is not bound by the sources, suggesting that the source concentration is not correct or that there is an outside source explaining the deviation (Figure 9. Figure A-5).

Specific conductivity and chloride were coupled in a 3-component mixing analysis and analyzed for a correlation with beetle-killed forest area. A positive correlation was observed between fractional groundwater contribution and beetle-killed forest area ($\rho=0.26$, $p = 0.43$) (Figure 7). This correlation was higher than that using either specific conductivity or chloride alone. While the correlation is not statistically significant, it reinforces the positive correlation observed using stable isotopes. Average source contribution at WCR indicates that streamflow is 51% groundwater, which is less than the estimation using isotopy (88%). The lower estimation from EMMA is due to the similarities between groundwater and surface water isotopic signatures. Both chloride and specific conductivity showed significant differences between groundwater and surface water concentrations for more of the watersheds.

Using a combination of chloride and specific conductivity, fractional groundwater contribution was calculated for each sampling date. The downstream site, WCR, displayed no evident temporal pattern (Figure 8). While it is expected that fractional groundwater contribution will increase after the cessation of snowmelt, this result is not evident using this tracer combination.

When EMMA was used to separate the fractional contribution of rain and snow, over half of the results gave values outside the acceptable range. This may result in part from the very chloride concentrations for snow and rain. The results from EMMA showed statistically significant correlation with the results from chloride ($\rho= 0.95$, $p<0.001$), but lower correlation with the results from specific conductivity ($\rho=0.42$, $p = 0.20$), indicating that chloride concentrations were more influential in end member mixing analysis (Figure A-6). The close values of chloride concentrations for snow (0.043 mg/L) and rain (0.040 mg/L) result in an inability to separate the fractional contribution of the two sources, making the results very similar to a two-component separation. In addition, the difference between groundwater, surface water, and precipitation chloride concentrations is on orders of magnitude. As a result, chloride has a greater influence on EMMA results than specific conductivity.

Watershed Physiography

Watershed characteristics (elevation, flow length, watershed area, baseflow discharge, slope, and time of concentration) were evaluated to determine physiographic effects on SGM. Mean watershed elevation was used to assess the effect of elevation on streamflow generation mechanisms. Total precipitation (Schermerhorn, 1967; Alpert, 1986) and SWE depth (Fassnacht et al., 2003) is affected by elevation. In addition, larger watersheds have been shown to display higher groundwater contributions to streamflow, due to regional scale sub-surface flow paths (Frisbee et al., 2011). Flow length and watershed area were assessed to examine this possibility. Baseflow in snowmelt-dominated watersheds is primarily groundwater fed (Miller et al., 2014), so total baseflow discharge was also used as a predictor for fractional groundwater contribution. Slope and time of concentration were compared to groundwater contribution because it is expected that an increased slope and decreased time of concentration might decrease deep infiltration.

These watershed characteristics were coupled with the results from the isotopic source separation. At the $\alpha=0.05$ level, no relation was significant (Table 6). However, at the $\alpha=0.10$ level, mean watershed elevation significantly negatively correlated with mean groundwater contribution (Figure 10). Mean watershed elevation is a better predictor of fractional groundwater contribution to streamflow than beetle-killed forest area. However, beetle-killed forest area and elevation are significantly negatively correlated ($\rho=-0.90$, $p=0.08$) for the 5 watersheds examined with isotopic composition, indicating that observed patterns in groundwater contribution may be partially explained by either predictor.

Table 6. Watershed characteristics and correlation with fractional groundwater contribution.

Characteristic	correlation (ρ)	p-value
Time of Concentration	0.4	0.52
Slope	-0.3	0.68
Area	0.7	0.23
Total baseflow	0.4	0.51
Average elevation	-0.9	0.08
Flow length	0.3	0.68

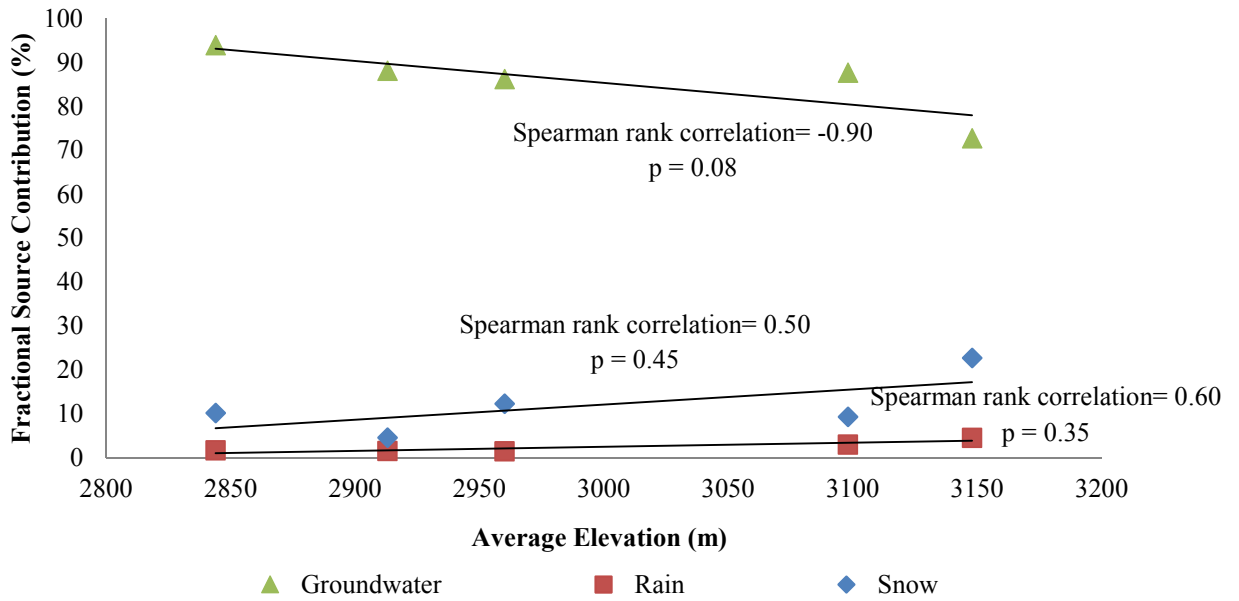


Figure 10. Fractional source contribution vs. elevation (m) for 5 watersheds in Willow Creek.

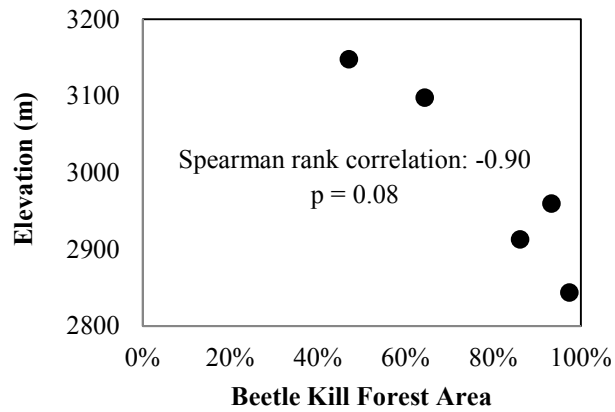


Figure 11. Mean elevation vs. beetle-killed forest area for 5 sub-watersheds assessed for isotopic composition.

CONCLUSIONS

The mountain pine beetle has resulted in widespread tree mortality in the Colorado Rocky Mountains. Four tracer methods were used to perform isotopic and chemical hydrograph separations to determine the effect of the mountain pine beetle on streamflow generation mechanisms (SGM). Using ^2H and ^{18}O isotopes of SGM water as tracers, groundwater contribution increased with increasing beetle-killed forest area ($\rho = 0.70$, $p = 0.23$). While not significant, this finding reinforces the results of other studies in the Colorado Rocky Mountains. Snow ($\rho=-0.60$) and rain ($\rho=-0.90$) were negatively correlated ($p = 0.35$ and 0.08). Snow and rain contribution decreased with increasing beetle-killed forest area. For rain, this correlation was statistically significant at the $\alpha=0.10$ level. Using specific conductivity to identify SGM, groundwater was negatively correlated with beetle-killed area ($\rho=-0.13$, $p=0.71$), indicating decreasing groundwater contribution with increasing beetle-killed forest area. Using chloride, groundwater was positively correlated with beetle-killed area ($\rho=0.19$, $p = 0.58$), and using EMMA, groundwater was positively correlated with beetle-killed area ($\rho=0.26$, $p = 0.43$).

None of the methods revealed statistically significant correlations between groundwater contribution and beetle-killed forest area. However, isotopy, chloride, and EMMA showed increasing groundwater contribution with increasing beetle kill forest area. Results for each method were not significantly correlated between each other, and stable isotopes showed systematically higher groundwater contribution estimations than previous studies and the chemical tracers due to closer similarities between groundwater and surface water compositions.

Individual watershed physiographic characteristics were assessed to determine if variables other than beetle-killed forest area affect streamflow generation mechanisms. Mean watershed elevation significantly correlated with fractional groundwater contribution when using isotopic tracers ($\rho=0.26$, $p = 0.43$). Mean elevation was also negatively correlated with beetle-killed forest area ($\rho=-0.90$, $p=0.08$).

RECOMMENDATIONS

It is recommended that a wider range of beetle-killed forest area is examined in future studies. While this study included frequent sampling events, the lowest value of beetle-killed forest area was 47% mortality. More information could be gained with several reference or undisturbed sites (beetle kill forest area < 15%). It is also recommended that more watersheds are sampled and assessed for isotope composition in order to increase statistical power.

It is recommended that several deeper groundwater wells are sampled for comparison to the shallow, riparian samples for higher confidence that the samples are representative of the groundwater. It is recommended that multiple samples be taken on each date at each site to assess for variability in data points, especially for groundwater samples. In addition, this will allow for a more robust comparison between sampling dates.

Continuous, *in-situ* measurement of specific conductivity could provide a comparison to grab samples and allow for continuous baseflow separation. This continuous measurement could also capture the behavior of streamflow generation mechanisms during melt events and summer storm events.

While chloride is a useful conservative tracer, low concentrations in end-member waters may decrease reliability of hydrograph separations. It is recommended that a variety of tracers (Calcium, Silica, Sodium, Magnesium, Sulfate, Potassium, etc.) are examined and chosen using principal component analysis before use in end member mixing equations in order to ensure that the tracers chosen account for the most amount of variability observed and that mixing diagrams show sources bounding streamflow well.

LITERATURE CITED

- Adams HD, Luce CH, Breshears DD, Allen CD, Weiler M, Hale VC, Smith AMS, and TE Huxman. 2012. Ecohydrological consequences of drought- and investment- triggered tree die-off: insights and hypotheses. *Ecohydrology*. 5:145-159.
- Alpert P. 1986. Mesoscale indexing of the distribution of orographic precipitation over high mountains. *Journal of Applied Meteorology and Climatology*. 25: 532-545.
- Ballard RG, Walsh MA, and WE Cole. 1984. The penetration and growth of blue-stain fungi in the sapwood of lodgepole pine attacked by mountain pine beetle. *Canadian Journal of Botany*. 62: 1724-1729.
- Bearup LA, Maxwell RM, Clow DW, and JE McCray. 2014. Hydrological effects of forest transpiration loss in bark beetle-impacted watersheds. *Nature Climate Change*. 4:481-486.
- Bergen JD. 1971. Vertical profiles of wind speed in a pine stand. *Forest Science*. 17(3):314-321.
- Bethlahmy N. 1974. More streamflow after a bark beetle epidemic. *Journal of Hydrology*. 23:185-189.
- Beudert B, Klocking B, and R Schwarze. 2007. Grosse Ohe: Impact of bark beetle infestation on the water and matter budget of a forested catchment. *Forest Hydrology Research Germany Russia*. 41-63.
- Biederman JA, Brook PD, Harpold AA, Gochis DJ, Gutmann E, Reed DE, Pendall E, and BE Ewers. 2012. Multiscale observations of snow accumulation and peak snowpack following widespread, insect-induced lodgepole pine mortality. *Ecohydrology*.
- Biederman JA, Harpold AA, Gochis DJ, Reed DE, Papagua SA, and PD Brooks. 2014. Increased evaporation following widespread tree mortality limits streamflow response. *Water Resources Research*. 50:5395 – 5409.
- Biederman JA, Somor AJ, Harpold AA, Gutmann ED, Breshears DD, Troch PA, Gochis DJ, Scott RL, Meddens AJH, and PD Brooks. 2015. Recent tree die-off has little effect on streamflow in contrast to expected increases from historical studies. *Water Resources Research*. 51: 9775-9789.
- Boon, S. 2011. Snow accumulation following forest disturbance. *Ecohydrology*. 5(3):279-285.
- Caissie D, Pollock TL, and RA Cunjak. 1996. Variation in stream water chemistry and hydrograph separation in a small drainage basin. *Journal of Hydrology*. 178:137-157.
- Chen F, Zhang G, Barlage M, Zhang Y, Hicke JA., Meddens A, Zhou G, Massman WJ, and J Frank. 2015. An Observational and Modeling Study of Impacts of Bark Beetle-Caused Tree Mortality on Surface Energy and Hydrological Cycles. *Journal of Hydrometeorology*. 16: 744-761.
- Christopherson N and RP Hooper. 1992. Multivariate Analysis of Stream Water Chemical Data: The Use of Principal Components Analysis for the End-Member Mixing Problem. *Water Resources Research*. 28(1):99-107.
- Clow DW, Rhoades C, Briggs J, Caldwell M, and WM Lewis. 2011. Responses of soil and water chemistry to mountain pine beetle induced tree mortality in Grand County, Colorado, USA. *Applied Geochemistry*. 26:S174-S178.

- Collins BJ, Rhoades CC, Hubbard RM, and MA Battaglia. 2011. Tree regeneration and future stand development after bark beetle infestation and harvesting in Colorado lodgepole pine stands. *Forest Ecology and Management*. 261:2168-2175.
- Colorado State Forest Service (CSFS). 2014. 2014 Colorado Forest Insect and Disease Update. Colorado State University Department of Natural Resources, Fort Collins, CO. As accessed 6 October 2015 at <https://csfs.colostate.edu/media/sites/22/2015/03/Final-2014-Insect-Disease-Update-2March2015.pdf>.
- Covino TP and BL McGlynn. 2007. Stream gains and losses across a mountain-to-valley transition: Impacts on watershed hydrology and stream water chemistry. *Water Resources Research*. 43: 1-14.
- Cox MH, Su GW, and J Constantz. 2007. Heat, chloride, and specific conductance as ground water tracers near streams. *Ground Water*. 45(2):187-195.
- Craig H. 1961. Isotopic Variations in Meteoric Waters. *Science*. 133:1702-1703.
- Dansgaard W. 1964. Stable Isotopes in Precipitation. *Tellus*. 16(4):436-468.
- Environmental Protection Agency (EPA). 1996. Method 9212: Potentiometric determination of Chloride in aqueous samples with ion-selective electrodes. Accessed 16 October 2015. <http://www3.epa.gov/epawaste/hazard/testmethods/sw846/pdfs/9212.pdf>
- Fassnacht SR, Dressler KA, and RC Bales. 2003. Snow water equivalent interpolation for the Colorado River Basin from snow telemetry (SNOTEL) data. *Water Resources Research*. 39 (8):1-10.
- Faure, G and TM Mensing. 2005. Isotopes: Principles and Applications. 3rd. Ed. *John Wiley and Sons*. Chapter 26.
- Feng, X, Taylor, S, Renchaw, CE, and JW Kirchner. 2002. Modeling isotopic evolution of snowmelt. *Water Resources Research*. 38(10):1-8.
- Frisbee MD, Phillips PF, Campbell AR, Liu F, and SA Sanchez. 2011. Streamflow generation in a large, alpine watershed in the southern Rocky Mountains of Colorado: Is streamflow generation simply the aggregation of hillslope runoff processes? *Water Resources Research*. 47(6): 1-18.
- Gat, JR. 2010. Isotope Hydrology: A Study of the Water Cycle. *Series on Environmental Science and Management*. 6.
- Grimaldi C, Thomas Z, Fossey M, Fauvel Y, and P Merot. 2009. High chloride concentrations in the soil and groundwater under an oak hedge in the West of France: an indicator of evapotranspiration and water movement. *Hydrological Processes* 23: 1865–1873.
- Gupta SK. 2010. Modern Hydrology and Sustainable Development. *John Wiley and Sons*. Chapter 7
- Harvey JW and KE Bencala. 1993. The effect of streambed topography on surface-subsurface water exchange in mountain catchments. *Water Resources Research*. 29(1):89-98.
- Hem JD. 1985. Study and Interpretation of the Chemical Characteristics of Natural Water. USGS Water Supply Paper 2254.
- Hermann A and W Stichler. 1981. Isotope input into runoff systems from melting snow covers. *Nordic Hydrology*. 12:30-9-318.

- Hooper RP and CA Shoemaker. 1986. A Comparison of Chemical and Isotopic Hydrograph Separation. *Water Resources Research*. 22(10):1444-1454.
- Hornbeck JW, Adams MB, Corbett ES, Verry ES, and JA Lynch. 1993. Long-term impacts of forest treatments on water yield: a summary for northeastern USA. *Journal of Hydrology*. 150:323-344
- Hornbeck JW, Martin CW, Eagar C. 1997. Summary of water yield experiments at Hubbard Brook experimental forest, New Hampshire. *Can J For Res*. 27:2043-2052.
- Hubbard RM, Rhoades CC, Elder K, and J Negron. 2013. Changes in transpiration and foliage growth in lodgepole pine trees following mountain pine beetle attack and mechanical girdling. *Forest Ecology and Management*. 289:312-317.
- Inger R, Jackson A, Parnell A, and S Bearhop. (nd). SIAR v4 – An ecologist’s guide. Accessed 15 Oct 2015 at http://mathsci.ucd.ie/~parnell_a/SIAR_For_Ecologists.pdf.
- Ingraham NL. 1998. Isotopic Variations in Precipitation. See Kendall & McDonnell, p 87-118.
- International Atomic Energy Agency (IAEA). 1997. Technical procedure for cumulative monthly sampling of precipitation for isotopic analysis. Available from: http://www-naweb.iaea.org/NAAL/HL/docs/tech_info/Precipitation%20Sampling97.pdf. Accessed 16 October 2015.
- Jobbagu EG and RB Jackson. 2007. Groundwater and soil chemical changes under phreatophytic tree plantations. *Journal of Geophysical Research*. 112:1-15.
- Kendall C and JJ McDonnell eds. 1988. *Isotope Tracers in Catchment Hydrology*. Amsterdam: Elsevier Science. 839 pp.
- Keppeler ET. 1998. The summer flow and water yield response to timber harvest. In: Ziemer, RR., technical coordinator. Proceedings of the conference on coastal watersheds: the Caspar Creek story, 6 May 1998; Ukiah, California. General Tech. Rep. PSW GTR-168. Albany, California: Pacific Southwest Research Station, Forest Service, U.S. Department of Agriculture: 35-43
- Kirchner JW, Tetzlaff D, and C Soulsby. 2010. Comparing chloride and water isotopes as hydrological tracers in two Scottish catchments. *Hydrological Processes*. 24:1631-1645.
- Klutsch JG, Negron JF, Costello SL, Rhoades CC, West DR, Popp J, and R Caissie. 2009. Stand characteristics and downed woody debris accumulations associated with a mountain pine beetle (*Dendroctonus ponderosae* Hopkins) outbreak in Colorado. *Forest Ecology and Management*. 258:641-649.
- Kronholm SC and PD Capel. 2015. A comparison of high-resolution specific conductance-based end-member mixing analysis and a graphical method for baseflow separation of four streams in hydrologically challenging agricultural watersheds. *Hydrological Processes*. 29:2521-2533.
- Kunkle GR. 1965. Computation of ground-water discharge to streams during floods, or to individual reaches during base flow, by use of specific conductance. USGS 525D Prof Paper. 207-210.
- Lewis KJ and ID Hartley. 2006. Rate of deterioration, degrade, and fall of trees killed by mountain pine beetle. *BC Journal of Ecosystems and Management* 7(2):11-19.

- Linveh B, Deems JS, Buma B, Barsugli JJ, Schneider D, Molotch NP, Wolter K, and CA Wessman. 2015. Catchment response to bark beetle outbreak and dust-on-snow in the Colorado Rocky Mountains. *Journal of Hydrology*. 523:196-210.
- Liu F, Williams MW, and N Caine. 2004. Source waters and flow paths in a n alpine catchment, Colorado Front Range, United States. *Water Resources Research*. 40:1-16.
- Love LD. 1955. The effects on stream flow of the killing of spruce and pine by the Engelmann Spruce beetle. *Transaction American Geophysical Union*. 36(1):113- 118.
- Maggart AL., 2014. Effects of mountain pine beetle caused tree mortality on streamflow and streamflow generation mechanisms in Colorado. Master's Thesis. Colorado State University, Fort Collins, CO. Accessed October 2015 from <http://hdl.handle.net/10217/82564>.
- Martin DA, Moody JA. 2001. Comparison of soil infiltration rates in burned and unburned mountainous watersheds. *Hydrological Processes* (15): 2893–2903.
- Menger AL. 2015. Response of streamflow and stream chemistry to pine beetle induced tree mortality across northern Colorado. Master's Thesis. Colorado State University, Fort Collins, CO. Accessed October 2015 from <https://dspace.library.colostate.edu/handle/10217/166963>.
- McDonald JH. 2014. Handbook of Biological Statistics (3rd ed.). Sparky House Publishing, Baltimore, Maryland. p 209-212.
- Miller MP, Susong DD, Shope CL, Heilweil VM, and BJ Stolp. 2014. Continuous estimation of baseflow in snowmelt-dominated streams and rivers in the Upper Colorado River Basin: A chemical hydrograph separation approach. *Water Resources Research*. 50:6986-6999.
- Mikkelson KM, Maxwell RM, Ferguson I, Stednick JD, McCray JE, and JO Sharp. 2013a. Mountain pine beetle infestation impacts: modeling water and energy budgets at the hill-slope scale. *Ecohydrology*. 6: 64-72.
- Mikkelson KM, Bearup LA, Maxwell RM, Stednick JD, McCray JE, and JO Sharp. 2013b. Bark beetle infestation impacts on nutrient cycling, water quality, and interdependent hydrological effects. *Biogeochemistry*. 115:1-21.
- Mitchell RG and Preisler HK. 1998. Fall rate of lodgepole pine killed by the mountain pine beetle in central Oregon. *Western Journal of Applied Forestry*. 13(1): 23-26.
- Moorehouse K, Johns T, Kaye J, and M Kaye. 2008. Carbon and nitrogen cycling immediately following bark beetle outbreaks in southwestern ponderosa pine forests. *Forest Ecology and Management*. 255: 2698-2708.
- Munyaneza O, Wenninger J, and S Uhlenbrook. 2012. Identification of runoff generation process using hydrometric and tracer methods in a meso-scale catchment in Rwanda. *Hydrology and Earth Sciences*. 16:1991-2004.
- Murray CD and JM Buttle, 2003. Impacts of clearcut harvesting on snow accumulation and melt in a northern hardwood forest. *Journal of Hydrology*. 271:197–212.
- Nakamura R. 1971. Runoff analysis by electrical conductance of water. *Journal of Hydrology*. 14:197-212.
- Nolan KM and RR Shields. 2000. *Measurement of stream discharge by wading*. US Geological Survey Water Resources Investigation Report 00 – 4036.

- Parnell A and A Jackson. 2015. SIAR: Stable Isotope Analysis in R (Version 4.2). [Software]. Available at <http://cran.r-project.org/web/packages/siar/index.html>.
- Perrot D, Molotch NP, Mussleman KN, and ET Pugh. 2014. Modelling the effects of the mountain pine beetle on snowmelt in a subalpine forest. *Ecohydrology*. 7:226-241.
- Peters NE and EB Radcliffe. 1998. Tracing hydrologic pathways using chloride at the Panola Mountain Research Watershed, Georgia, USA. *Water, Air, and Soil Pollution*. 105:263-275.
- Phillips DL and JW Gregg. 2003. Source partitioning using stable isotopes: coping with too many sources. *Oecologia*. 136:261-269.
- Pilgrim DH, Huff DD, and TD Steele. 1979. Use of Specific Conductance and Contact Time Relations for Separating Flow Components in Storm Runoff. *Water Resources Research*. 15(2):329-339.
- Pinder GF, and JF Jones. 1969. Determination of the Ground-Water Component of Peak Discharge from the Chemistry of Total Runoff. *Water Resources Research*. 5(2):438-445.
- Potts DF. 1984. Hydrologic impacts of a large-scale mountain pine beetle (*Dendroctonus Ponderosae* Hopkins) epidemic. *Water Resources Bulletin*. 20(3):373-377.
- Pugh E and E Gordon. 2013. A conceptual model of water yield effects from beetle induced tree death in snow-dominated lodgepole pine forests. *Hydrological Processes*. 27: 2048-2060.
- Pugh E and E Small. 2012. The impact of pine beetle infestation on snow accumulation and melt in the headwaters of the Colorado River. *Ecohydrology* 5: 467-477.
- Pugh E and EE Small. 2013. The impact of beetle-induced conifer death on stand-scale canopy snow interception. *Hydrology Research*. 44(4):644-657.
- Raffa KF, Aukema BH, Bentz BJ, Carroll AL, Hicke JA, Turner MG, and WH Romme. 2008. Cross-scale drivers of natural disturbances prone to anthropogenic amplification: The dynamics of bark beetle eruptions. *BioScience*. 58(6): 501-517.
- Rice KC and Hornberger GM. 1988. Comparison of hydrochemical tracers to estimate source contributions to peak flow in a small, forested, headwater catchment. *Water Resources Research*. 34(7):1755-1766.
- Roth BE, Slatton KC, and MJ Cohen. 2007. On the potential for high-resolution lidar to improve rainfall interception estimates in forest ecosystems. *Front Ecol Environ*. 5:421-428
- Schermerhorn VP. 1967. Relations between topography and annual precipitation in western Oregon and Washington. *Water Resources Research*. 3(3): 707-711
- Sklash MG and RN Farvolden. 1979. The role of groundwater in storm runoff. *Journal of Hydrology*. 43:45-65.
- Space ML, Ingraham N L, and JW Hess. 1991. The use of stable isotopes in quantifying groundwater discharge to a partially diverted creek. *Journal of Hydrology*. 129:175-193.
- Stednick JD. 1996. Monitoring the effects of timber harvest on annual water yield. *Journal of Hydrology*. 76:79-95.

- Sun G, McNulty SG, Shepard JP, Amatya DM, Riekerk H, Comerford NB, Skaggs W and L Swift. 2001. Effects of timber management on the hydrology of wetland forests in the southern United States. *Forest Ecology & Management*. 143:227–236.
- Surfleet CG and AE Skaugset. 2013. The effect of timber harvest on summer low flows, Hinkle Creek, Oregon. *West Journal of Applied Forestry*. 28 (1): 13-21.
- Taylor S, Feng X, Renshaw C, and E Kirchner. 2001. Isotopic evolution of snowmelt: Validation and parameterization of a one-dimensional model using controlled snowmelt experiments. *Water Resources Research*. 37:759-769.
- Troendle CA and King RM. 1985. The effect of clear cutting and timber harvest on the Fool Creek watershed, 30 years later. *Water Resources Research*. 21(12): 1915-22.
- Troendle CA and King RM. 1987. The effect of partial and clearcutting on streamflow at Deadhorse Creek, Colorado. *Journal of Hydrology*. 90: 145-57.
- Troendle CA and Reuss JO. 1997. Effect of clearcutting on snow accumulation and water outflow at Fraser, Colorado. *Hydrology and Earth Systems Science*. 1(2): 325-332.
- University of Wyoming Stable Isotope Facility (UWYSIF). Available from: <http://www.uwyo.edu/sif/> Accessed 11 May 2015.
- USDA. 2014. Aerial Detection Survey [Data file]. Retrieved from http://www.fs.usda.gov/detail/r2/forest-grasslandhealth/?cid=fsbdev3_041629
- USGS Land Cover Institute. 2005. Conifer Forest Layer [Data file] Retrieved from <http://landcover.usgs.gov/nalcms.php>
- USGS National Elevation Dataset. 2013. The National Map [Data file] Retrieved from <http://nationalmap.gov/elevation.html>
- Vogt T, Hoehn H, Schneider P, Freund A, Shirmer M, and OA Cirpka. 2010. Fluctuations of electrical conductivity as a natural tracer for bank filtration in a losing stream. *Advances in Water Resources*. 33: 1296-1308.
- Wessa P. 2015. Free Statistics Software, Office for Research Development and Education, version 1.1.23-r7, URL: <http://www.wessa.net/>
- Winter TC, Harvey JW, Franke OL and WM Alley. 1998. Ground Water and Surface Water: A Single Resource. *U.S. Geol. Surv. Circular 1139*
- Wulder MA, White JC, Bentz B, Alvarez MF, and NC Coops. 2006. Estimating the probability of mountain pine beetle red-attack damage. *Remote Sensing of Environment*. 101: 150-166.
- Zeman LJ and HO Slaymaker. 1975. Hydrochemical analysis to discriminate variable runoff source areas in an alpine basin. *Arctic and Alpine Research*. 7(4):34

APPENDIX

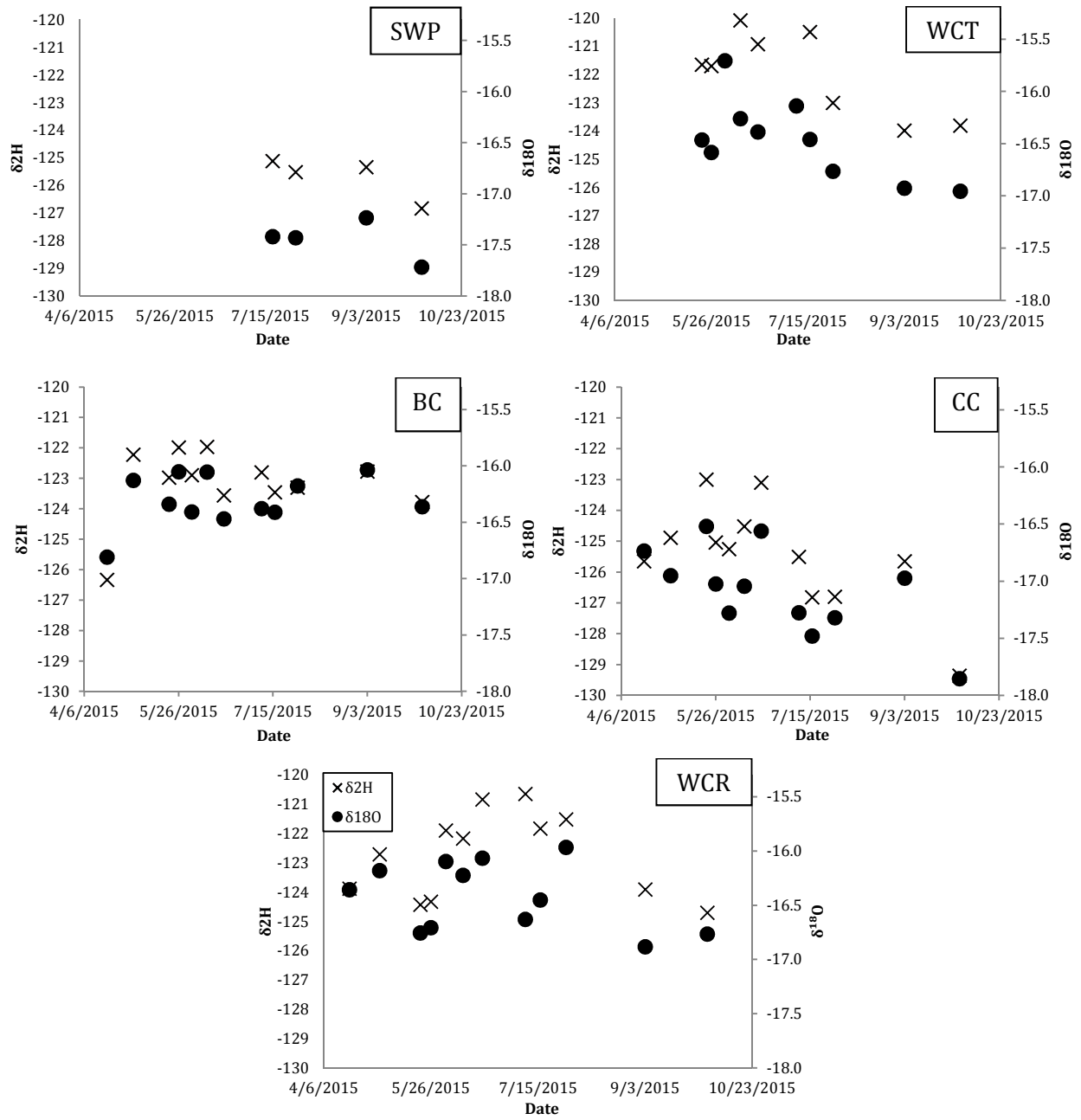
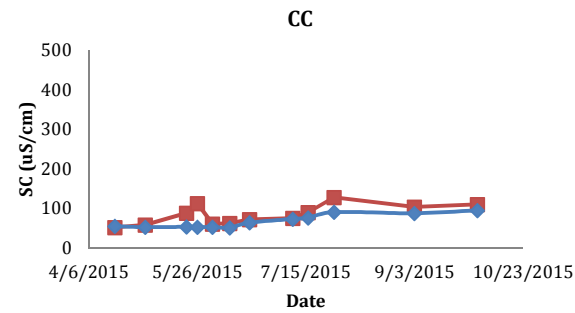
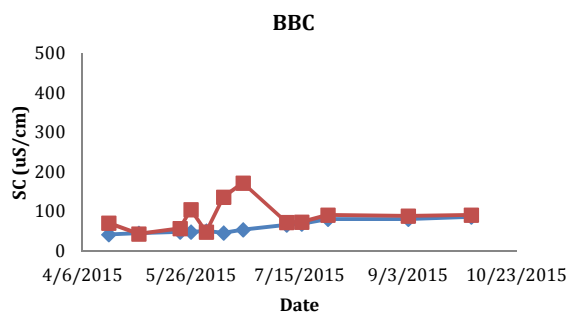
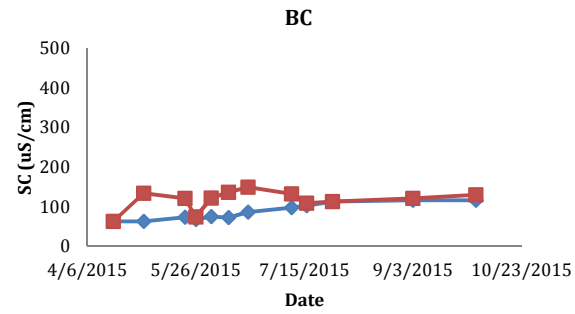
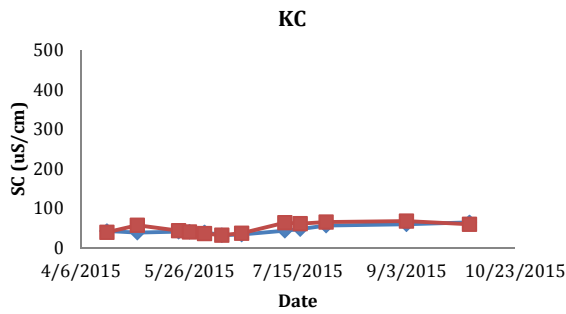
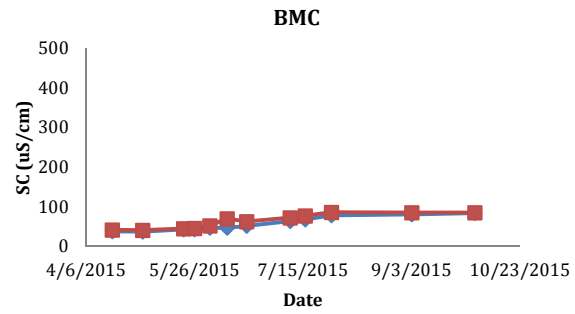
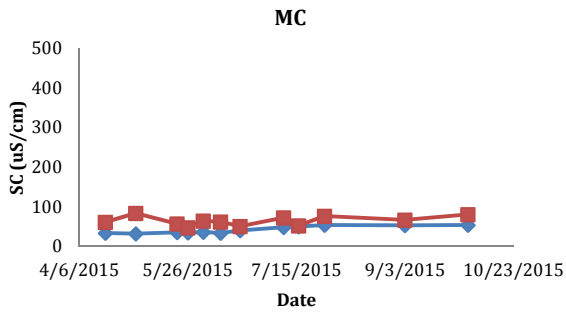
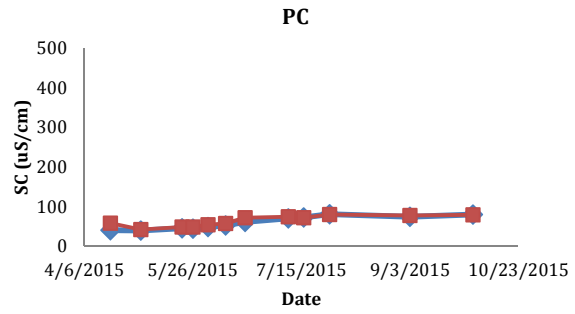
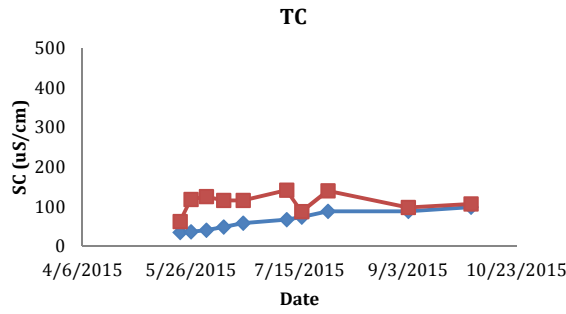
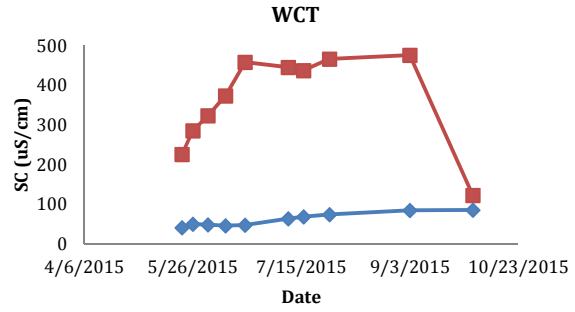
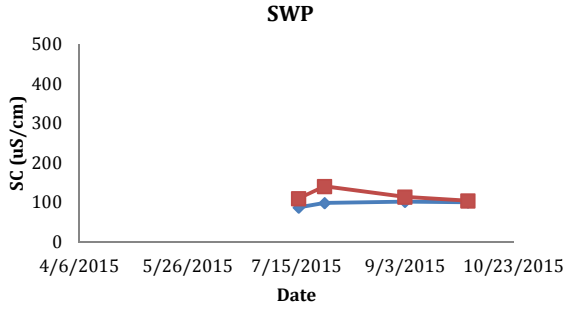


Figure A-1. Stream water isotope composition over time for sampling dates between April 2015 and October 2015.



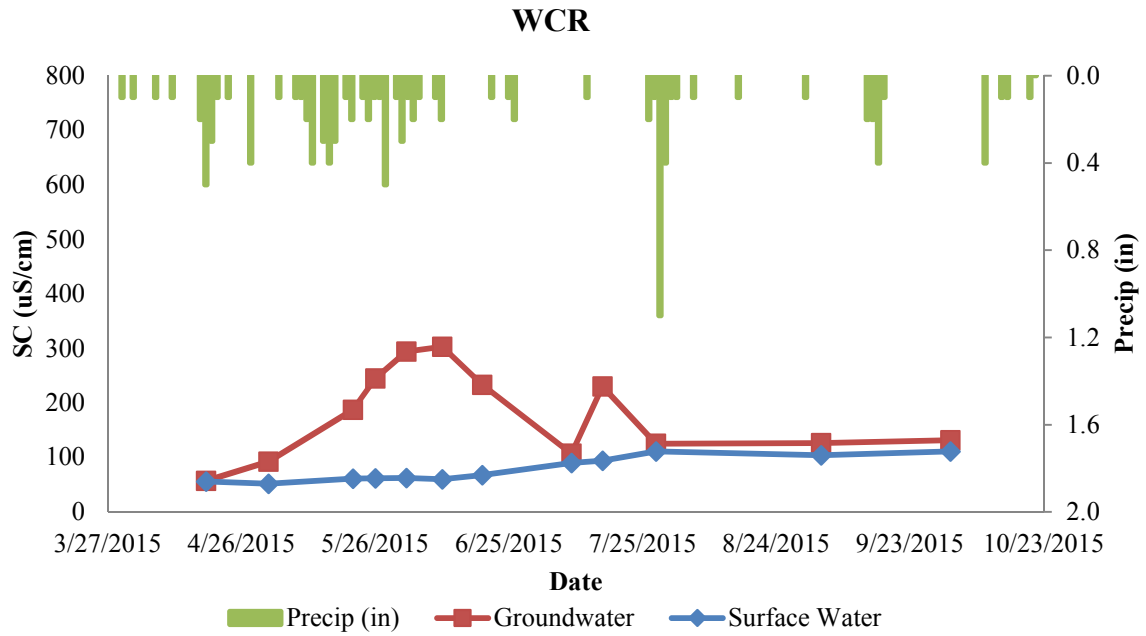
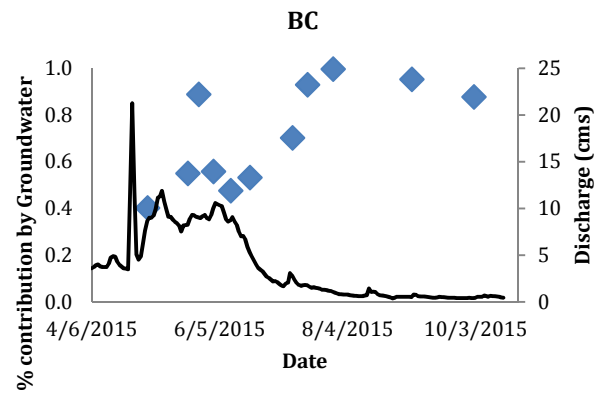
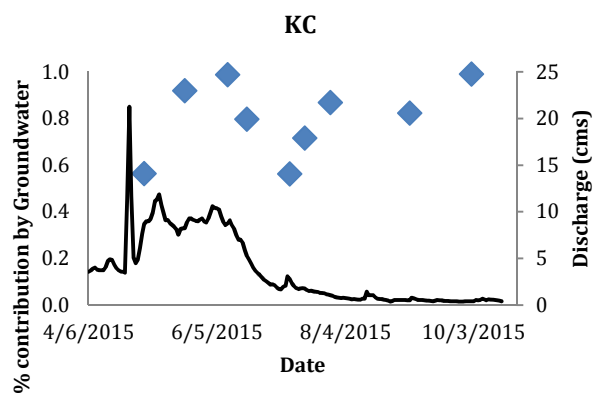
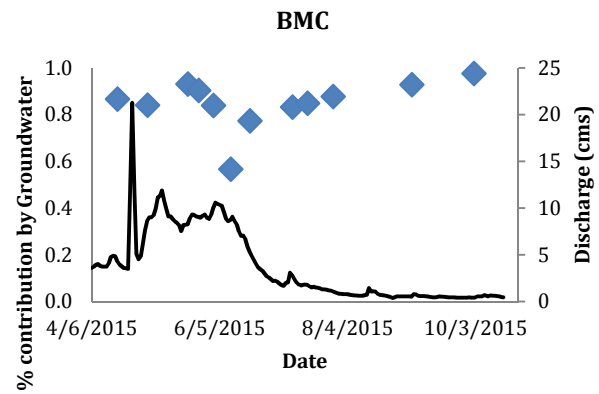
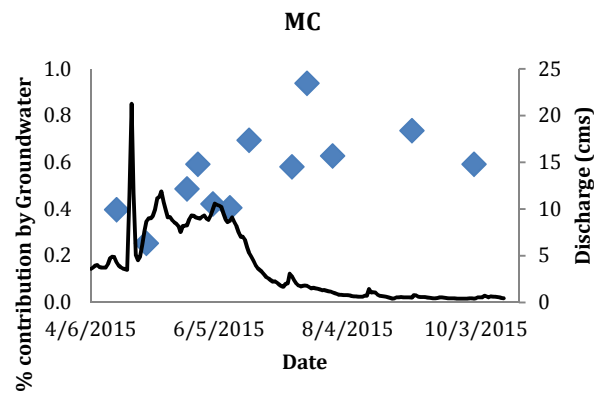
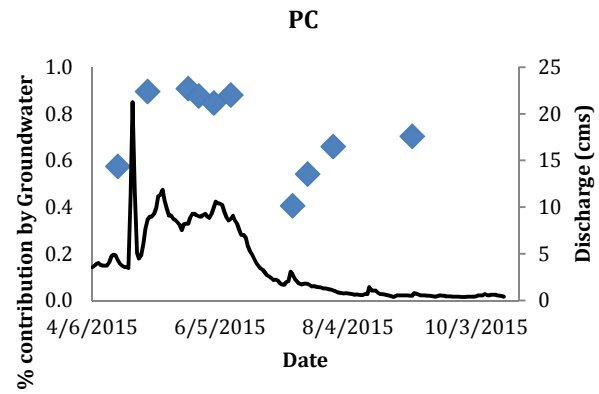
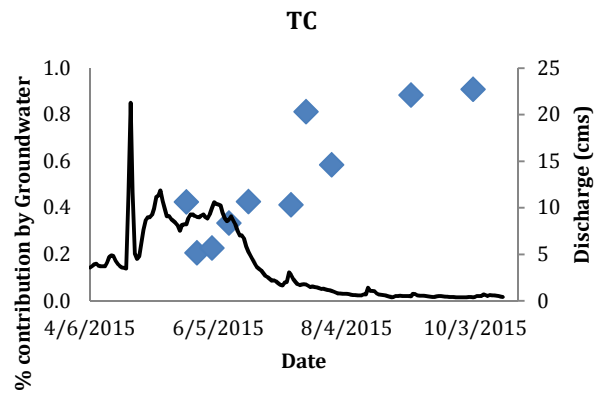
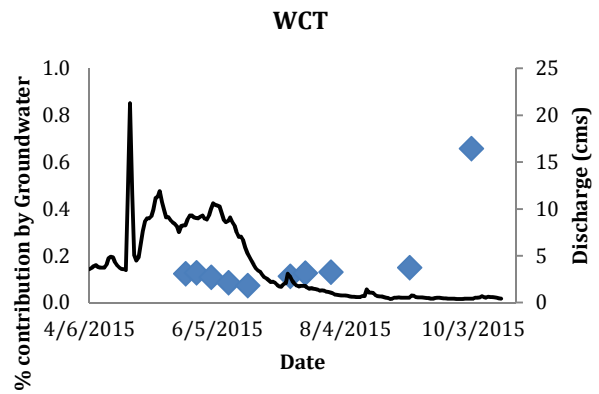
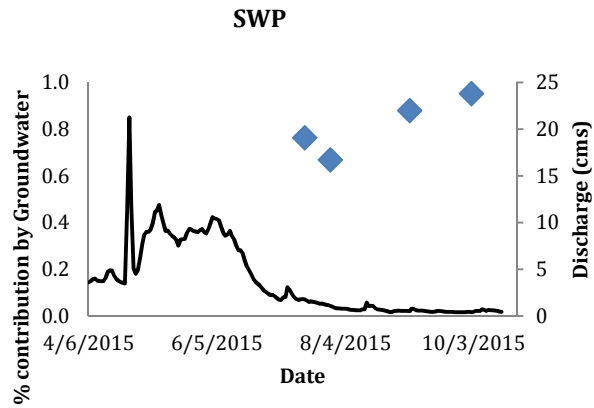


Figure A-2. Groundwater and surface water specific conductivity ($\mu\text{S}/\text{cm}$) at each sampling date for each site data from GRAND LAKE 6 SSW station (<http://www.ncdc.noaa.gov/>).



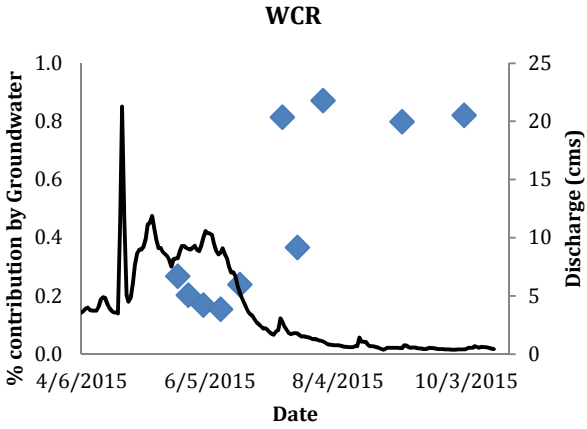
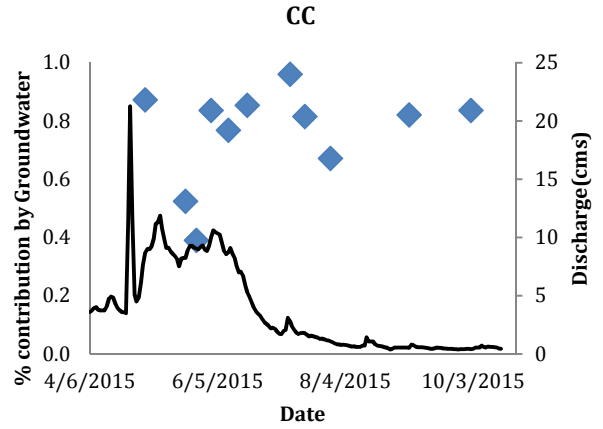
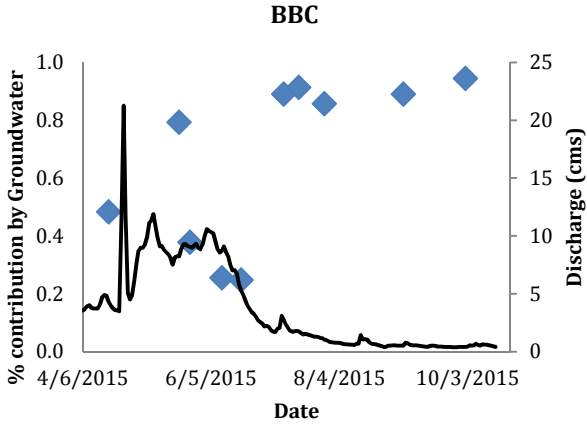
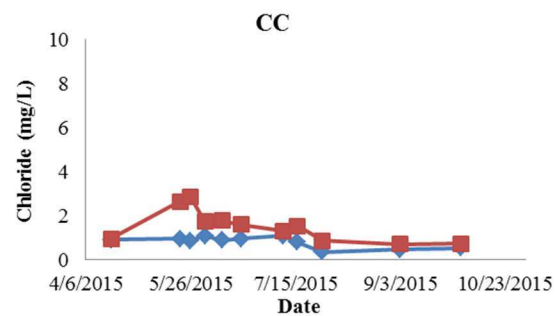
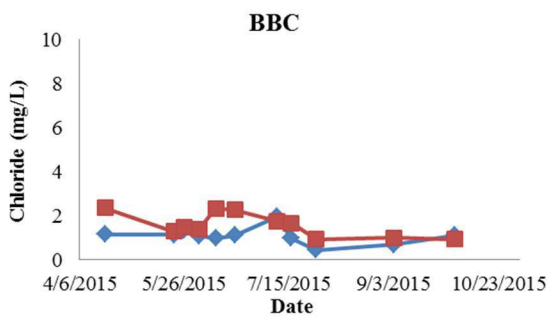
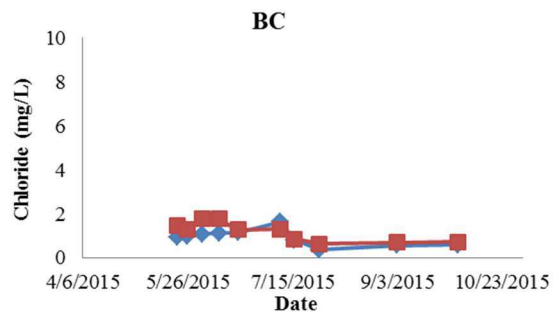
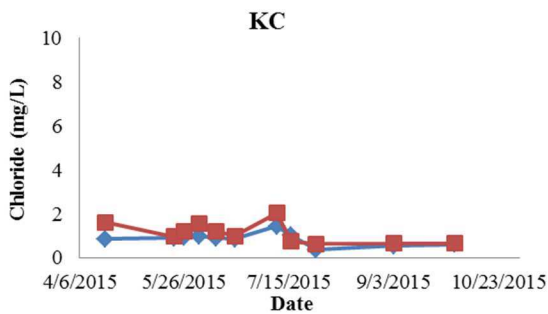
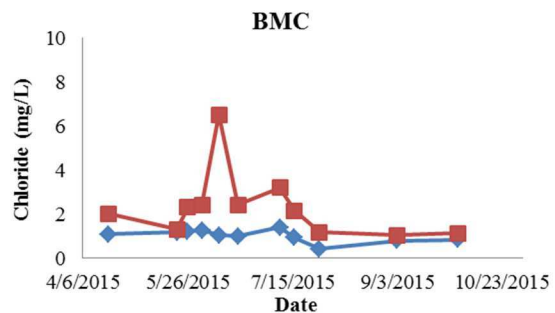
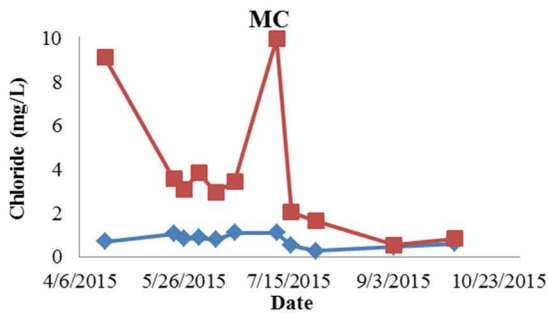
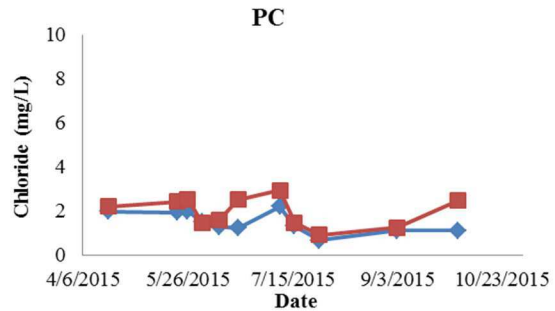
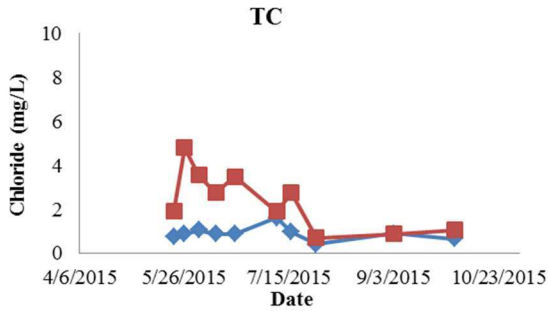
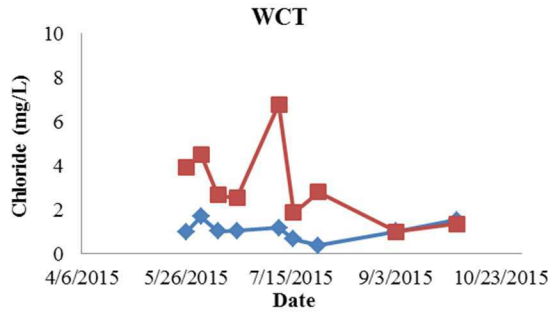
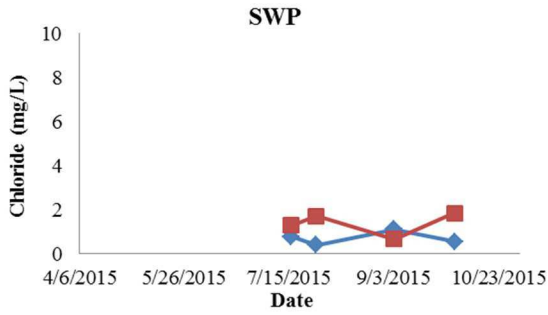


Figure A-3. Groundwater contribution for each sampling date at each sampling site based on specific conductivity.



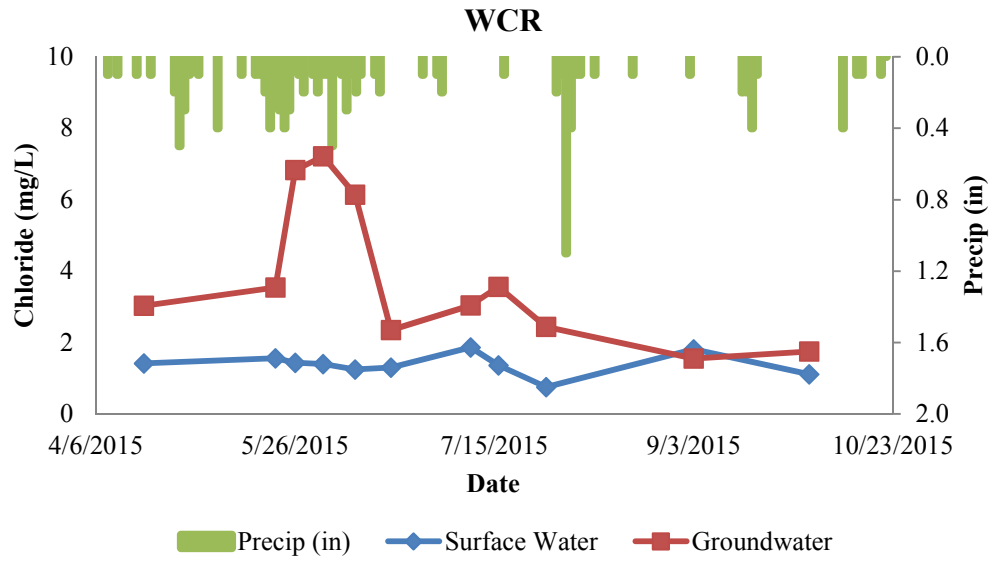


Figure A-4. Groundwater and surface water chloride (mg/L) at each sampling date for each site.

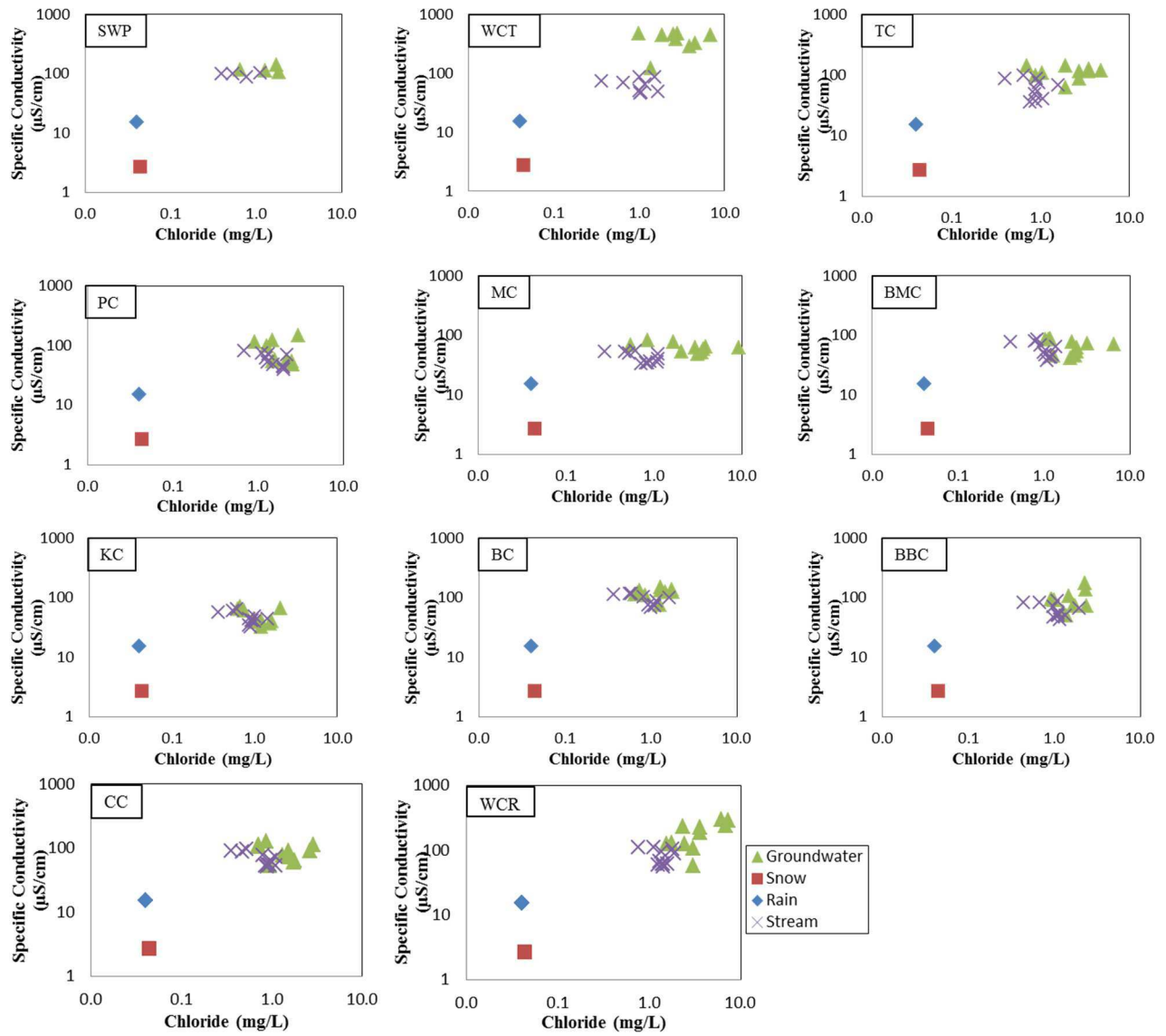


Figure A-5. Mixing diagrams showing source (groundwater, snow, rain) and specific conductivity vs. chloride concentrations.

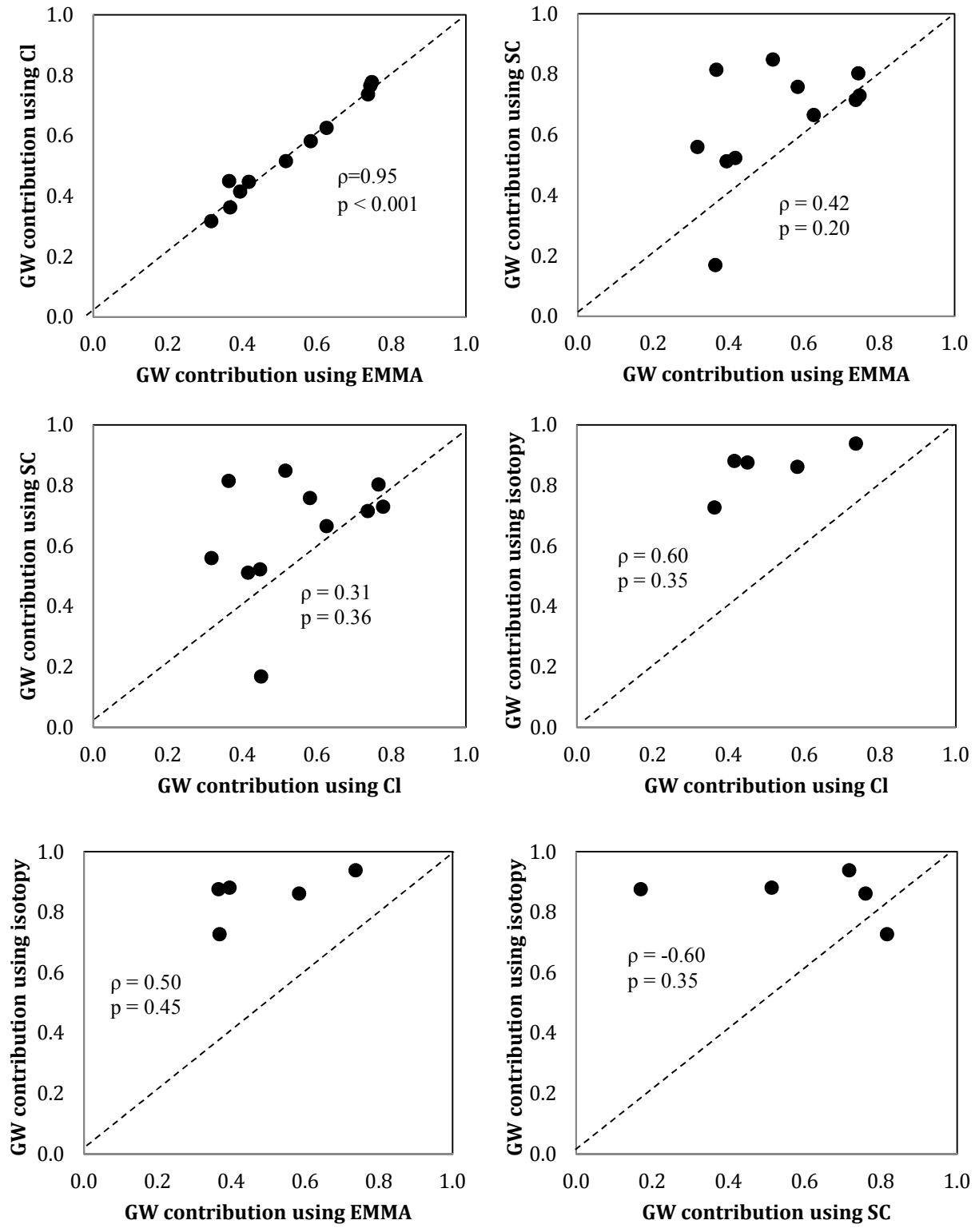


Figure A-6. Correlation between groundwater contribution results for all different methods used.

Table A-1. Sampling dates for study watersheds and sample parameters obtained for each date. Symbols correspond to chloride (†), specific conductivity (❖), isotopes (■), and discharge (⊙).

Site	18-Apr	2-May	21-May	26-May	2-Jun	10-Jun	19-Jun	9-Jul	16-Jul	28-Jul	3-Sep	2-Oct
SWP									❖†■	❖†■⊙	❖†■⊙	❖†■
WCT			❖†■	❖†■	❖†■	❖†■	❖†■	❖†■⊙	❖†■⊙	❖†■⊙	❖†■⊙	❖†■
TC			❖†	❖†	❖†	❖†	❖†	❖†⊙	❖†⊙	❖†⊙	❖†⊙	❖†
PC	❖†	❖†	❖†	❖†	❖†	❖†	❖†	❖†⊙	❖†⊙	❖†⊙	❖†⊙	❖†
MC	❖†	❖†	❖†	❖†	❖†	❖†	❖†	❖†⊙	❖†⊙	❖†⊙	❖†⊙	❖†
BMC	❖†	❖†	❖†	❖†	❖†	❖†	❖†	❖†⊙	❖†⊙	❖†⊙	❖†⊙	❖†
KC	❖†	❖†	❖†	❖†	❖†	❖†	❖†	❖†⊙	❖†⊙	❖†⊙	❖†⊙	❖†
BC	❖†■	❖†■	❖†■	❖†■	❖†■	❖†■	❖†■	❖†■⊙	❖†■⊙	❖†■⊙	❖†■⊙	❖†■
BBC	❖†	❖†	❖†	❖†	❖†	❖†	❖†	❖†⊙	❖†⊙	❖†⊙	❖†⊙	❖†
CC	❖†■	❖†■	❖†■	❖†■	❖†■	❖†■	❖†■	❖†■⊙	❖†■⊙	❖†■⊙	❖†■⊙	❖†■
WCR	❖†■	❖†■	❖†■	❖†■	❖†■	❖†■	❖†■	❖†■	❖†■	❖†■	❖†■	❖†■

Table A-2. Specific conductivity and chloride data by sample site, date, and type.

Site	Sampling Date	Type	Specific Conductivity ($\mu\text{S}/\text{cm}$)	Chloride (mg/L)
BBC	4/18/2015	Groundwater	71.7	2.349
BC	4/18/2015	Groundwater	63.1	
BMC	4/18/2015	Groundwater	41.5	2.026
CC	4/18/2015	Groundwater	52.6	0.937
KC	4/18/2015	Groundwater	39.4	1.625
MC	4/18/2015	Groundwater	61.3	9.145
PC	4/18/2015	Groundwater	58.6	2.205
WCR	4/18/2015	Groundwater	57.3	3.029
WCP	4/18/2015	Snow	2.7	
BBC	4/18/2015	Stream	42.5	1.154
BC	4/18/2015	Stream	63.4	0.883
BMC	4/18/2015	Stream	38.0	1.092
CC	4/18/2015	Stream	55.1	0.910
KC	4/18/2015	Stream	43.2	0.865
MC	4/18/2015	Stream	33.4	0.706
PC	4/18/2015	Stream	40.1	2.000
WCR	4/18/2015	Stream	56.0	1.413
BBC	5/2/2015	Groundwater	44.0	
BC	5/2/2015	Groundwater	133.9	
BMC	5/2/2015	Groundwater	40.9	
CC	5/2/2015	Groundwater	58.3	
KC	5/2/2015	Groundwater	57.5	
MC	5/2/2015	Groundwater	83.4	
PC	5/2/2015	Groundwater	42.3	
WCR	5/2/2015	Groundwater	92.1	
BBC	5/2/2015	Stream	45.4	
BC	5/2/2015	Stream	62.9	
BMC	5/2/2015	Stream	36.8	
CC	5/2/2015	Stream	52.8	
KC	5/2/2015	Stream	39.0	
MC	5/2/2015	Stream	32.3	
PC	5/2/2015	Stream	39.5	
WCR	5/2/2015	Stream	51.5	
BBC	5/21/2015	Groundwater	57.7	1.271
BC	5/21/2015	Groundwater	121.6	1.456
BMC	5/21/2015	Groundwater	44.6	1.299
CC	5/21/2015	Groundwater	88.8	2.645
KC	5/21/2015	Groundwater	44.0	0.978
MC	5/21/2015	Groundwater	57.2	3.588
PC	5/21/2015	Groundwater	48.2	2.441

Site	Sampling Date	Type	Specific Conductivity (µS/cm)	Chloride (mg/L)
TC	5/21/2015	Groundwater	62.4	1.909
WCR	5/21/2015	Groundwater	187.2	3.542
WCT	5/21/2015	Groundwater	226.0	
BBC	5/21/2015	Stream	48.9	1.120
BC	5/21/2015	Stream	73.7	0.941
BMC	5/21/2015	Stream	42.6	1.168
CC	5/21/2015	Stream	53.7	0.937
KC	5/21/2015	Stream	41.7	0.910
MC	5/21/2015	Stream	35.5	1.078
PC	5/21/2015	Stream	45.2	1.950
TC	5/21/2015	Stream	35.2	0.775
WCR	5/21/2015	Stream	61.2	1.565
WCT	5/21/2015	Stream	41.0	0.880
BBC	5/26/2015	Groundwater	105.7	1.475
BC	5/26/2015	Groundwater	74.5	1.277
BMC	5/26/2015	Groundwater	45.5	2.310
CC	5/26/2015	Groundwater	112.8	2.830
KC	5/26/2015	Groundwater	40.8	1.203
MC	5/26/2015	Groundwater	47.4	3.107
PC	5/26/2015	Groundwater	48.4	2.557
TC	5/26/2015	Groundwater	117.9	4.785
WCR	5/26/2015	Groundwater	245.0	6.828
WCT	5/26/2015	Groundwater	286.0	3.921
BBC	5/26/2015	Stream	49.4	1.338
BC	5/26/2015	Stream	67.9	0.995
BMC	5/26/2015	Stream	42.6	1.224
CC	5/26/2015	Stream	53.1	0.850
KC	5/26/2015	Stream	41.4	0.937
MC	5/26/2015	Stream	34.2	0.847
PC	5/26/2015	Stream	44.3	2.026
TC	5/26/2015	Stream	36.4	0.887
WCR	5/26/2015	Stream	61.7	1.432
WCT	5/26/2015	Stream	49.5	0.999
BBC	6/2/2015	Groundwater	49.3	1.366
BC	6/2/2015	Groundwater	122.5	1.792
BMC	6/2/2015	Groundwater	52.4	2.420
CC	6/2/2015	Groundwater	60.8	1.725
KC	6/2/2015	Groundwater	36.8	1.545
MC	6/2/2015	Groundwater	64.6	3.888
PC	6/2/2015	Groundwater	54.4	1.487
TC	6/2/2015	Groundwater	125.7	3.557

Site	Sampling Date	Type	Specific Conductivity (µS/cm)	Chloride (mg/L)
WCR	6/2/2015	Groundwater	294.0	7.215
WCT	6/2/2015	Groundwater	324.0	4.509
BBC	6/2/2015	Stream	51.8	1.078
BC	6/2/2015	Stream	75.1	1.092
BMC	6/2/2015	Stream	46.4	1.266
CC	6/2/2015	Stream	53.3	1.092
KC	6/2/2015	Stream	39.8	0.999
MC	6/2/2015	Stream	35.9	0.895
PC	6/2/2015	Stream	48.4	1.500
TC	6/2/2015	Stream	40.4	1.069
WCR	6/2/2015	Stream	62.2	1.396
WCT	6/2/2015	Stream	48.5	1.674
BBC	6/10/2015	Groundwater	137.3	2.320
BC	6/10/2015	Groundwater	136.6	1.762
BMC	6/10/2015	Groundwater	70.0	6.518
CC	6/10/2015	Groundwater	62.9	1.762
KC	6/10/2015	Groundwater	32.3	1.208
MC	6/10/2015	Groundwater	61.9	2.953
PC	6/10/2015	Groundwater	57.5	1.598
TC	6/10/2015	Groundwater	115.4	2.759
WCR	6/10/2015	Groundwater	303.0	6.143
WCT	6/10/2015	Groundwater	374.0	2.667
WCP	6/10/2015	Rain	21.6	
BBC	6/10/2015	Stream	46.4	0.974
BC	6/10/2015	Stream	73.0	1.120
BMC	6/10/2015	Stream	46.2	1.046
CC	6/10/2015	Stream	51.8	0.887
KC	6/10/2015	Stream	32.1	0.906
MC	6/10/2015	Stream	34.0	0.801
PC	6/10/2015	Stream	52.5	1.304
TC	6/10/2015	Stream	48.7	0.876
WCR	6/10/2015	Stream	59.7	1.250
WCT	6/10/2015	Stream	45.8	1.020
BBC	6/19/2015	Groundwater	173.0	2.261
BC	6/19/2015	Groundwater	149.8	1.288
BMC	6/19/2015	Groundwater	62.4	2.420
CC	6/19/2015	Groundwater	72.5	1.598
KC	6/19/2015	Groundwater	37.6	1.003
KC-2	6/19/2015	Groundwater	40.5	
MC	6/19/2015	Groundwater	50.7	3.468
PC	6/19/2015	Groundwater	71.7	2.516

Site	Sampling Date	Type	Specific Conductivity (µS/cm)	Chloride (mg/L)
PC-2	6/19/2015	Groundwater	36.0	
TC	6/19/2015	Groundwater	115.6	3.483
WCR	6/19/2015	Groundwater	233.0	2.349
WCT	6/19/2015	Groundwater	459.0	2.535
WCP	6/19/2015	Rain	39.0	
BBC	6/19/2015	Stream	54.4	1.106
BC	6/19/2015	Stream	86.8	1.154
BMC	6/19/2015	Stream	51.7	1.003
CC	6/19/2015	Stream	64.1	0.957
KC	6/19/2015	Stream	34.2	0.865
MC	6/19/2015	Stream	39.8	1.115
PC	6/19/2015	Stream	61.3	1.245
TC	6/19/2015	Stream	58.1	0.883
WCR	6/19/2015	Stream	67.3	1.299
WCT	6/19/2015	Stream	47.3	1.046
BBC	7/9/2015	Groundwater	73.0	1.748
BC	7/9/2015	Groundwater	133.0	1.294
BMC	7/9/2015	Groundwater	72.8	3.203
CC	7/9/2015	Groundwater	75.8	1.310
KC	7/9/2015	Groundwater	64.2	3.079
KC-2	7/9/2015	Groundwater	68.7	1.017
MC	7/9/2015	Groundwater	72.3	10.008
PC	7/9/2015	Groundwater	74.4	2.948
PC-2	7/9/2015	Groundwater	227.0	
TC	7/9/2015	Groundwater	141.4	1.915
WCR	7/9/2015	Groundwater	107.1	3.042
WCT	7/9/2015	Groundwater	446.0	6.765
WCP	7/9/2015	Rain	7.0	
BBC	7/9/2015	Stream	66.7	1.94
BC	7/9/2015	Stream	97.9	1.63
BMC	7/9/2015	Stream	63.2	1.39
CC	7/9/2015	Stream	73.4	1.09
KC	7/9/2015	Stream	44.0	1.43
MC	7/9/2015	Stream	48.3	1.11
PC	7/9/2015	Stream	70.2	2.21
TC	7/9/2015	Stream	67.4	1.61
WCR	7/9/2015	Stream	90.0	1.86
WCT	7/9/2015	Stream	63.7	1.17
BBC	7/16/2015	Groundwater	74.5	1.663
BC	7/16/2015	Groundwater	109.1	0.851
BMC	7/16/2015	Groundwater	77.0	2.146

Site	Sampling Date	Type	Specific Conductivity (µS/cm)	Chloride (mg/L)
CC	7/16/2015	Groundwater	90.5	1.521
KC	7/16/2015	Groundwater	61.7	0.754
KC-2	7/16/2015	Groundwater	59.5	
MC	7/16/2015	Groundwater	52.3	2.062
PC	7/16/2015	Groundwater	72.3	1.472
PC-2	7/16/2015	Groundwater	170.3	
SWP	7/16/2015	Groundwater	110.5	1.272
TC	7/16/2015	Groundwater	87.0	2.745
WCR	7/16/2015	Groundwater	230.0	3.557
WCT	7/16/2015	Groundwater	438.0	1.869
WCP	7/16/2015	Rain	12.9	
BBC	7/16/2015	Stream	69.4	0.973
BC	7/16/2015	Stream	102.6	0.821
BMC	7/16/2015	Stream	67.7	0.918
CC	7/16/2015	Stream	76.6	0.799
KC	7/16/2015	Stream	47.7	1.004
MC	7/16/2015	Stream	50.0	0.523
PC	7/16/2015	Stream	72.8	1.324
SWP	7/16/2015	Stream	87.9	0.775
TC	7/16/2015	Stream	73.6	0.973
WCR	7/16/2015	Stream	93.9	1.360
WCT	7/16/2015	Stream	68.4	0.648
BBC	7/28/2015	Groundwater	91.9	0.916
BC	7/28/2015	Groundwater	113.3	0.643
BMC	7/28/2015	Groundwater	86.5	1.179
CC	7/28/2015	Groundwater	128.1	0.865
KC	7/28/2015	Groundwater	65.5	0.627
KC-2	7/28/2015	Groundwater	60.9	0.639
MC	7/28/2015	Groundwater	76.5	1.659
PC	7/28/2015	Groundwater	80.4	0.823
PC-2	7/28/2015	Groundwater	148.8	1.026
SWP	7/28/2015	Groundwater	140.9	1.712
TC	7/28/2015	Groundwater	139.6	0.702
WCR	7/28/2015	Groundwater	125.1	2.440
WCT	7/28/2015	Groundwater	467.0	2.804
BBC	7/28/2015	Stream	81.0	0.434
BC	7/28/2015	Stream	113.1	0.369
BMC	7/28/2015	Stream	77.8	0.408
CC	7/28/2015	Stream	90.9	0.355
KC	7/28/2015	Stream	56.9	0.362
MC	7/28/2015	Stream	53.6	0.276

Site	Sampling Date	Type	Specific Conductivity (µS/cm)	Chloride (mg/L)
PC	7/28/2015	Stream	80.8	0.685
SWP	7/28/2015	Stream	99.2	0.395
TC	7/28/2015	Stream	88.0	0.405
WCR	7/28/2015	Stream	111.0	0.758
WCT	7/28/2015	Stream	73.7	0.359
BBC	9/3/2015	Groundwater	89.2	0.990
BC	9/3/2015	Groundwater	121.0	0.706
BMC	9/3/2015	Groundwater	85.1	1.037
CC	9/3/2015	Groundwater	103.9	0.698
KC	9/3/2015	Groundwater	68.3	0.615
KC-2	9/3/2015	Groundwater	71.6	0.718
MC	9/3/2015	Groundwater	66.9	0.542
PC	9/3/2015	Groundwater	77.9	1.204
PC-2	9/3/2015	Groundwater	119.9	1.335
SWP	9/3/2015	Groundwater	114.5	0.651
TC	9/3/2015	Groundwater	97.6	0.888
WCR	9/3/2015	Groundwater	126.4	1.551
WCT	9/3/2015	Groundwater	477.0	0.990
WCP	9/3/2015	Rain	6.9	
BBC	9/3/2015	Stream	81.1	0.678
BC	9/3/2015	Stream	116.1	0.567
BMC	9/3/2015	Stream	80.1	0.787
CC	9/3/2015	Stream	88.0	0.464
KC	9/3/2015	Stream	60.3	0.548
MC	9/3/2015	Stream	53.2	0.466
PC	9/3/2015	Stream	74.1	1.117
SWP	9/3/2015	Stream	102.5	1.100
TC	9/3/2015	Stream	88.1	0.904
WCR	9/3/2015	Stream	104.1	1.813
WCT	9/3/2015	Stream	84.3	1.007
BBC	10/2/2015	Groundwater	91.6	0.936
BC	10/2/2015	Groundwater	130.2	0.736
BMC	10/2/2015	Groundwater	85.2	1.125
CC	10/2/2015	Groundwater	110.7	0.715
KC	10/2/2015	Groundwater	60.1	0.664
KC-2	10/2/2015	Groundwater	69.8	0.844
MC	10/2/2015	Groundwater	80.9	2.480
PC	10/2/2015	Groundwater	79.5	1.830
SWP	10/2/2015	Groundwater	104.7	1.056
TC	10/2/2015	Groundwater	106.8	1.748
WCR	10/2/2015	Groundwater	131.6	1.359

Site	Sampling Date	Type	Specific Conductivity (µS/cm)	Chloride (mg/L)
WCT	10/2/2015	Groundwater	122.5	2.334
BBC	10/2/2015	Stream	87.4	1.093
BC	10/2/2015	Stream	116.2	0.592
BMC	10/2/2015	Stream	83.6	0.830
CC	10/2/2015	Stream	95.1	0.525
KC	10/2/2015	Stream	64.5	0.616
MC	10/2/2015	Stream	54.0	0.613
PC	10/2/2015	Stream	80.1	1.502
SWP	10/2/2015	Stream	100.4	1.200
TC	10/2/2015	Stream	98.6	0.869
WCR	10/2/2015	Stream	110.8	1.112
WCT	10/2/2015	Stream	85.7	1.112

Table A-3. Discharge (m³/s) at each site by sample date.

Site	Sampling Date	Discharge (m ³ /s)
BBC	7/9/15	1.75
BBC	7/16/15	1.20
BBC	7/28/15	0.82
BBC	9/3/15	0.36
BC	7/9/15	0.09
BC	7/16/15	0.05
BC	7/28/15	0.03
BC	9/3/15	0.02
BMC	7/9/15	1.02
BMC	7/16/15	0.93
BMC	7/28/15	0.49
BMC	9/3/15	0.25
CC	7/9/15	0.15
CC	7/16/15	0.08
CC	7/28/15	0.09
CC	9/3/15	0.06
KC	7/9/15	0.18
KC	7/16/15	0.16
KC	7/28/15	0.06
KC	9/3/15	0.03
MC	7/9/15	0.03
MC	7/16/15	0.02
MC	7/28/15	0.02
MC	9/3/15	0.01
PC	7/9/15	0.21
PC	7/16/15	0.15
PC	7/28/15	0.09
PC	9/3/15	0.06
SWP	7/28/15	0.03
SWP	9/3/15	0.01
TC	7/9/15	0.06
TC	7/16/15	0.06
TC	7/28/15	0.01
TC	9/3/15	0.01
WCR	7/9/15	2.81
WCR	7/16/15	1.77
WCR	7/28/15	1.06
WCR	9/3/15	0.51
WCT	7/9/15	0.90
WCT	7/16/15	0.50
WCT	7/28/15	0.24
WCT	9/3/15	0.12

Table A-4. Isotopic composition of samples by sample site, date, and type for ^2H and ^{18}O (‰).

Site	Sampling Date	Type	$\delta^2\text{H}$ (‰)	$\delta^{18}\text{O}$ (‰)
BC	4/18/15	Groundwater	-125	-16.6
BC	5/2/15	Groundwater	-124	-16.8
BC	5/21/15	Groundwater	-124	-16.6
BC	5/26/15	Groundwater	-122	-16.2
BC	6/2/15	Groundwater	-123	-16.2
BC	6/10/15	Groundwater	-123	-16.2
BC	6/19/15	Groundwater	-120	-15.5
BC	7/9/15	Groundwater	-123	-16.3
BC	7/16/15	Groundwater	-122	-16.1
BC	7/28/15	Groundwater	-124	-16.5
BC	9/3/15	Groundwater	-122	-15.6
BC	10/2/15	Groundwater	-123	-16.2
BC	4/18/15	Stream	-126	-16.8
BC	5/2/15	Stream	-122	-16.1
BC	5/21/15	Stream	-123	-16.3
BC	5/26/15	Stream	-122	-16.1
BC	6/2/15	Stream	-123	-16.4
BC	6/10/15	Stream	-122	-16.1
BC	6/19/15	Stream	-124	-16.5
BC	7/9/15	Stream	-123	-16.4
BC	7/16/15	Stream	-123	-16.4
BC	7/28/15	Stream	-123	-16.2
BC	9/3/15	Stream	-123	-16.0
BC	10/2/15	Stream	-124	-16.4
CC	4/18/15	Groundwater	-125	-16.5
CC	5/2/15	Groundwater	-125	-17.0
CC	5/21/15	Groundwater	-123	-16.6
CC	5/26/15	Groundwater	-122	-16.5
CC	6/2/15	Groundwater	-124	-16.9
CC	6/10/15	Groundwater	-125	-17.1
CC	6/19/15	Groundwater	-125	-17.2
CC	7/9/15	Groundwater	-123	-16.6
CC	7/16/15	Groundwater	-124	-17.2
CC	7/28/15	Groundwater	-120	-16.5
CC	9/3/15	Groundwater	-122	-16.7
CC	10/2/15	Groundwater	-120	-16.5
CC	4/18/15	Stream	-126	-16.7
CC	5/2/15	Stream	-125	-16.9
CC	5/21/15	Stream	-123	-16.5
CC	5/26/15	Stream	-125	-17.0
CC	6/2/15	Stream	-125	-17.3
CC	6/10/15	Stream	-125	-17.0
CC	6/19/15	Stream	-123	-16.6
CC	7/9/15	Stream	-126	-17.3

Site	Sampling Date	Type	$\delta^2\text{H}$ (‰)	$\delta^{18}\text{O}$ (‰)
CC	7/16/15	Stream	-127	-17.5
CC	7/28/15	Stream	-127	-17.3
CC	9/3/15	Stream	-126	-17.0
CC	10/2/15	Stream	-129	-17.9
SWP	7/16/15	Groundwater	-119	-16.6
SWP	7/28/15	Groundwater	-122	-16.6
SWP	9/3/15	Groundwater	-126	-17.4
SWP	10/2/15	Groundwater	-125	-17.4
SWP	7/16/15	Stream	-125	-17.4
SWP	7/28/15	Stream	-126	-17.4
SWP	9/3/15	Stream	-125	-17.2
SWP	10/2/15	Stream	-127	-17.7
WCP	6/10/15	Rain	-101	-13.6
WCP	6/19/15	Rain	-77	-10.4
WCP	7/9/15	Rain	-66	-10.0
WCP	7/16/15	Rain	-49	-7.2
WCP	9/3/15	Rain	-45	-7.4
WCP	4/18/15	Snow	-152	-20.4
WCR	4/18/15	Groundwater	-121	-16.0
WCR	5/2/15	Groundwater	-121	-16.2
WCR	5/21/15	Groundwater	-123	-15.9
WCR	5/26/15	Groundwater	-120	-15.9
WCR	6/2/15	Groundwater	-118	-15.4
WCR	6/10/15	Groundwater	-119	-15.5
WCR	6/19/15	Groundwater	-123	-16.9
WCR	7/9/15	Groundwater	-119	-16.4
WCR	7/16/15	Groundwater	-117	-15.5
WCR	7/28/15	Groundwater	-123	-16.6
WCR	9/3/15	Groundwater	-121	-16.3
WCR	10/2/15	Groundwater	-124	-16.7
WCR	4/18/15	Stream	-124	-16.4
WCR	5/2/15	Stream	-123	-16.2
WCR	5/21/15	Stream	-124	-16.8
WCR	5/26/15	Stream	-124	-16.7
WCR	6/2/15	Stream	-122	-16.1
WCR	6/10/15	Stream	-122	-16.2
WCR	6/19/15	Stream	-121	-16.1
WCR	7/9/15	Stream	-121	-16.6
WCR	7/16/15	Stream	-122	-16.4
WCR	7/28/15	Stream	-122	-16.0
WCR	9/3/15	Stream	-124	-16.9
WCR	10/2/15	Stream	-125	-16.8
WCT	5/26/15	Groundwater	-120	-16.3
WCT	6/2/15	Groundwater	-118	-15.7
WCT	6/10/15	Groundwater	-120	-16.4

Site	Sampling Date	Type	$\delta^2\text{H}$ (‰)	$\delta^{18}\text{O}$ (‰)
WCT	6/19/15	Groundwater	-121	-16.6
WCT	7/9/15	Groundwater	-120	-16.4
WCT	7/16/15	Groundwater	-120	-16.3
WCT	7/28/15	Groundwater	-119	-16.1
WCT	9/3/15	Groundwater	-121	-16.8
WCT	10/2/15	Groundwater	-123	-16.8
WCT	5/21/15	Stream	-122	-16.5
WCT	5/26/15	Stream	-122	-16.6
WCT	6/2/15	Stream	-118	-15.7
WCT	6/10/15	Stream	-120	-16.3
WCT	6/19/15	Stream	-121	-16.4
WCT	7/9/15	Stream	-118	-16.1
WCT	7/16/15	Stream	-120	-16.5
WCT	7/28/15	Stream	-123	-16.8
WCT	9/3/15	Stream	-124	-16.9
WCT	10/2/15	Stream	-124	-17.0